JCTC Journal of Chemical Theory and Computation

Article

pubs.acs.org/JCTC

Structure, Energy, and Vibrational Frequencies of Oxygen Allotropes O_n ($n \leq 6$) in the Covalently Bound and van der Waals Forms: Ab Initio Study at the CCSD(T) Level

Oleg B. Gadzhiev,*[,†,‡,⊥] Stanislav K. Ignatov,*[,§,∥,⊥] Mikhail Yu. Kulikov,[†,∥] Alexander M. Feigin,[†] Alexey G. Razuvaev,[§] Peter G. Sennikov,[‡] and Otto Schrems[∥]

[†]Institute of Applied Physics, Russian Academy of Sciences, Nizhny Novgorod, 46 Ul'yanov Street, Nizhny Novgorod, 603950, Russia

[‡]G.G. Devyatykh Institute of Chemistry of High Purity Substances, Russian Academy of Sciences, 49 Troponina St., Nizhny Novgorod, 603950, Russia

[§]N.I. Lobachevsky State University of Nizhny Novgorod, National Research University, 23 Gagarin Avenue, Nizhny Novgorod, 603950, Russia

[∥]Alfred Wegener Institute for Polar and Marine Research, Am Handelshafen 12, 27570 Bremerhaven, Germany

Supporting Information

ABSTRACT: Recent experiments on the UV and electron beam irradiation of solid O_2 reveals a series of IR features near the valence antisymmetric vibration band of O_3 which are frequently interpreted as the formation of unusual O_n allotropes in the forms of weak complexes or covalently bound molecules. In order to elucidate the question of the nature of the irradiation products, the structure, relative energies, and vibrational frequencies of various forms of O_n (n = 1−6) in the singlet, triplet, and, in some cases, quintet states were studied using the CCSD(T) method up to the CCSD(T,full)/cc-pCVTZ and CCSD(T,FC)/aug-cc-pVTZ levels. The results of calculations demonstrate the existence of stable highly symmetric structures O_4 (D_{3h}), O_4 (D_{2d}), and O_6 (D_{3d}) as well as the intermolecular complexes $O_2 \cdot O_2$, $O_2 \cdot O_3$, and $O_3 \cdot O_3$ in different conformations. The calculations show that the local minimum corresponding to the $O_3 \cdots O$ complex is quite shallow and cannot explain the ν_3 band features close to 1040 cm^{-1}, as was proposed previously. For the ozone dimer, a new conformer was found which is more stable than the structure known to date. The effect of the ozone dimer on the registered IR spectra is discussed.

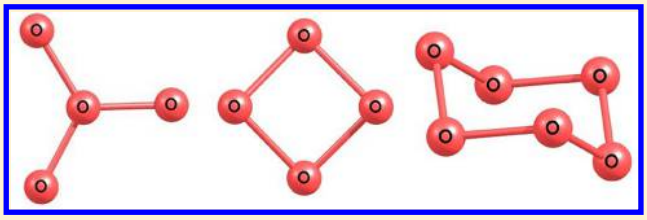

1. INTRODUCTION

The existence of the higher neutral allotropic forms of oxygen O_n (n > 3) is an intriguing and fundamental question in inorganic and physical chemistry. The idea about the existence of O_4 dates back to early works of Dolezalek and then Lewis[1,2] to possibly explain the magnetic properties of liquid oxygen. In the end of the 1970s, the influence of the complexes $(O_2)_2$ on the energy balance in the atmosphere attracted the attention of spectroscopists. In 1980, Adamantides et al.[3,4] studied theoretically for the first time the covalently bound allotropic form of tetraoxygen O_4, establishing that the molecule has a cyclic structure of D_{2d} symmetry. Later, Røggen and Nilssen[5] demonstrated that the "pinwheel" D_{3h} structure of O_4 is also stable, although less energetically favorable than the cyclic isomer. The studies of tetraoxygen were continued in theoretical studies.[6−24] Among them, the most fundamental results were obtained by Seidl and Schaefer,[7,8] who investigated the thermodynamic and kinetic stability of cyclic O_4 (up to the CCSD(T)/DZP level) including the transition states and activation energies of the O_4 dissociation, and more recently by Hernandez-Lamoneda and Ramirez-Solis,[16,17] who obtained high-level data for the O_4 structure and energy using the CCSD(T)/aug-cc-pVQZ and CASSCF(16,12)-ACPF//CASSCF(16,12)-RS2 methods. These values were also confirmed by Caffarel et al.[25] who reported the energy of O_4 calculated using the multireference quantum Monte Carlo theory. This theory can potentially account for a greater amount of electronic correlation than the CCSD(T) method. It follows from these works that O_4 can exist in two singlet-state isomeric forms: cyclic puckered D_{2d} and open planar D_{3h} structures. The energy of the D_{2d} structure relatively to O_2 ($^3\Sigma_g^-$) is ~93−95[17] or 98.5 ± 1.9[22] kcal/mol; the energy of the D_{3h} structure is about 116.2 kcal/mol (value obtained in refs 26 and 27 at the CCSD(T)/TZ2P level). The activation barrier of dissociation of the cyclic structure to $2O_2$ is estimated to be in the range of 6.6−9.3 kcal/mol[17] or 11.6 ± 1.6 kcal/mol.[22] Such remarkable activation barrier height stimulated attempts of experimental detection of covalently bound O_4. The first experimental observation was reported by Bevsek et al.,[28] who formed O_4 by DC discharge and O_3 photolysis observing the REMPI spectrum assigned to O_4 of the D_{2d} structure. Later,

Received: July 27, 2012
Published: November 16, 2012

   dx.doi.org/10.1021/ct3006584 | J. Chem. Theory Comput. 2013, 9, 247−262

Peterka et al.[26,27] reported an O_4 observation on the basis of the rotationally resolved photoionization spectra, photoelectron spectra (combined with *ab initio* calculations) which were considered "strong evidence of metastable O_4*." The last statement was then questioned by Chestakov et al.,[29] who concluded that the spectrum observed in refs 26 and 27 appears due to impurities of iron ions in the experimental setup. The most recent detection of O_4 was reported by Cacace et al.[30] on the basis of a neutralization-recharging beam technique combined with mass spectrometry.

It should also be noted that the van der Waals oxygen dimer $(O_2)_2$, which is also termed frequently as O_4 or tetraoxygen, was also intensively studied both theoretically and experimentally. It was observed experimentally both in the low-temperature matrix[31,32] and in the molecular beams.[33] The most recent theoretical studies of intermolecular complexes $(O_2)_2$, $(O_2)_4$, and $(O_2)_3$ are presented in refs 34−36 where high-level *ab initio* and quantum Monte Carlo methods are applied in the investigations for material sciences. The clusters $(O_2)_4$ are of particular importance for the oxygen solid state at extremely high pressure.[37,38] The giant clusters $(O_2)_N$ with several thousands of O_2 molecular units are potentially important for future technologies based on a relatively new concept called "chemistry with a hammer."[34,39,40] A polymeric form of oxygen (θ-O_4 phase based on a polymeric chain structural motif) was predicted in ref 41 on the basis of DFT calculations.

Although rather complete and detailed information has now been obtained concerning the existence of tetraoxygen, the covalently bound hexaoxygen O_6 molecule is studied to a much lesser extent. For the first time, the covalently bound structure of O_6 was considered theoretically by Blahous and Schaefer[42] and later by Xie et al.[43] in the search of "high energy density materials," i.e., materials which can be used as prospective fuels, propellants, and explosives. It was shown that O_6 molecule has a D_{3d} "chair" structure similar to cyclohexane. In ref 42, only the SCF/STO-3G, DZ, and DZP structure was reported, augmented by frequency calculations. In ref 43, the geometry parameters, IR frequencies, and Raman intensities were studied for the D_{3d} structure of O_6 using the SCF and MP2 theories in the DZP and TZ2P bases. In 1990s, attention was given to O_6 in the series of works of Gimarc and Zhao,[44−47] who investigated the question of strain energy of the inorganic cyclic compounds from the point of view of structural chemistry. In these works, the structures and energies of O_6 were studied on the MP2/6-31G* level along with the structures of other oxygen cycles O_n. Later, the DFT and MP2 theories were applied to O_4, O_6, O_8, and O_{12}.[18] In that work, the stable structure of O_6 (and also O_8) was not found at the DFT level (B3LYP and B3PW91 with conjunction 6-31G* and 6−311G(2df) basis sets) but was optimized using the MP2 calculations, although the corresponding energies and structural data were not reported. In the experimental and theoretical study of Probst et al.,[48] it was also reported that MP2/6-311G* calculations were performed for O_6 (and MP2/DZP for O_8) without detailed presentation of the calculation data. In 2002, there was a report[49] that the O_6 and O_9 ozone clusters were optimized at the PM3 level and using the MP4/6-311++G(d,p) and QCISD/6-311++G(d,p) potential curve calculations. The ozone dimerization energy estimated here was approximately 1 kcal/mol; however, the structure of the ozone dimer was rather different from that obtained earlier by Slanina.[50,51]

Thus, there is a lack of information concerning the covalently bound hexaoxygen O_6. Moreover, the data on the structure, binding energies, and the vibrational frequencies of the ozone van der Waals dimer were obtained a long time ago using a level of theory which is not appropriate for the needs of the present day. Namely, it is not clear whether the structure of the dimer observed in the inert matrix by Schriver et al.[52] corresponds to the structure considered by Slanina.[50,51]

In the middle of 1990s, experiments on the UV irradiation of the solid oxygen films conducted in different laboratories raised a question about the possible formation of unusual forms of the oxygen species or complexes in atmospheric ice particles or in space oxygen-rich ice bodies. Namely, in the associated works,[52,53] the changes in IR spectra of the solid oxygen and oxygen in an argon matrix after UV irradiation were interpreted as a formation of complexes between O_3 and atomic oxygen. This fact can have significant effects on the current atmospheric models[54] and deserve special attention. First, the question is whether the observed results can be interpreted as an O_3···O complex. If yes, what are its thermodynamic and spectral properties, spin state, structure, and reactivity? If not, the second question is what species or effects are responsible for the changes in IR spectra observed experimentally? In particular, the question is whether it is possible to describe the observed effects by the formation of oxygen complexes or, probably, other oxygen allotropes.

Therefore, the present work is devoted to the quantum chemical study of the structure, energy, and spectral characteristics of both covalently bound and van der Waals structures of oxygen allotropes O_n $(4 < n < 6)$, which can, in principle, be responsible for the observed IR features. Hereafter, we will use the term "bound" for the molecular structures where all the atoms have one or more internuclear distance not longer than 2.5 Å. The species with the elongated contacts (with typical van der Waals O···O distances 3−5 Å) will be referenced hereafter as "molecular complexes."

The goal of this study is to obtain reliable data on the structure, energy of formation, and vibrational frequencies of polyoxygen in the forms of both a covalently bound molecule and a weakly bound complex in order to make assignments for the infrared bands observed in the solid oxygen irradiation experiments and, thus, a decision on the natures of the species formed during such irradiation. In this case, the frequency calculations and determination IR-shift for the polyoxygen substances at the theory level for the high-correlated method.

In the beginning of the present work, we will make an extensive benchmark of the single reference coupled cluster methodology for the smallest oxygen substances, including the O atoms and O_2 and O_3 molecules. Next, we will consider the O_4 molecules with an extended CAS(24,16) active space. It is the first one which can describe reliably both (cyclic and open) isomers and provide the correct reference functions for the MRCI calculations. The chain form of the tetraoxygen is investigated at the coupled cluster and CASSCF theory levels. Further, we will present results for O_5 and O_6 molecular units, and later for atomic-molecular and pure molecular complexes calculated at the high-correlated theory levels and verified by the multireference approach.

2. CALCULATION DETAILS

The main computational part was performed at the CCSD and CCSD(T) levels of theory using the cc-pVTZ, aug-cc-pVTZ, and cc-pCVTZ basis sets. cc-pCVTZ is a special kind of basis

set augmented by tight core functions.[55,56] The importance of core−core and core−valence correlation for high precision calculations was demonstrated in ref 57 (see also refs 58 and 59). As it was shown, the use of the core functions in CCSD(T) calculations remarkably improves the geometry parameters and harmonic frequencies of ozone molecule. We considered this level the most reliable and tried to use it for the geometry optimization and frequency calculation of all the species under consideration. In some cases, however, the calculations on that level were impossible, either because of convergence problems or because the molecule was not stable at this level. In that case, we report the results obtained at lower levels. For the molecular complexes, we also tried to take into account the long-range effects using the basis set augmented by diffuse functions (CCSD(T,FC)/aug-cc-pVTZ).

The CCSD and CASSCF calculations were carried out using the Gaussian 03 program.[60] The Firefly QC package,[61] which is partially based on the GAMESS (US) source code,[62] was used for the preliminary search for stationary points at different levels of the CASSCF method. For the CCSD(T) calculations, the program CFOUR[63,64] was used, which allows for geometry optimizations with analytic gradients[65,66] and analytic second derivatives for frequency calculations.[67,68] Full geometry optimization was performed for all the systems, typically followed by frequency calculations. For the geometry optimizations, several starting points were examined, especially for the flexible structures of molecular complexes. In addition, the MRCI energy calculations were carried out for the O_4 molecules and their production from O_2. The cyclic O_5 was optimized at the strongly contracted NEVPT2/cc-pVTZ theory level with numerical evaluation of gradients. To reduce computational time, the resolution of identity (RI) approximation with an auxiliary cc-pVTZ/C basis set was employed. All the multi-reference calculations beyond CASSCF were carried out with the ORCA suite of programs.[69] For the coupled cluster calculation beyond CCSD(T), the MRCC program[70,71] interfaced to the CFOUR suite of programs was used. The internal test of the single reference coupled cluster methodology was carried out with the focal point analysis[72−74] methodology for singlet−triplet splitting of the O atom, the O_2 molecule (up to CCSDTQ), and the gap between open and closed O_3 (up to CCSDT(Q)).

For visualization and initial structure preparation, the GaussView03,[75] ChemCraft,[76] and Moltran[77] graphical programs were employed.

3. RESULTS AND DISCUSSION

Atomic Oxygen, Molecular Oxygen, and Ozone. Electronic structures and physical and chemical properties of the dioxygen substances have been excellently reviewed in ref 78 and more recently.[79] Table 1S (see Supporting Information) presents the calculated energies of atomic oxygen $O(^3P)$ and $O(^1D)$, as well as the energies, geometry parameters, and harmonic vibrational frequencies of molecular oxygen $O_2(X^3\Sigma_g^-)$ and $O_2(a^1\Delta_g)$ and ozone O_3 $(\tilde{X}^1A_1)$ at the CCSD/cc-pVTZ level and with the CCSD(T) method in conjunction with basis sets up to aug-cc-pV5Z. These oxygen substances are the reference systems to assess the chosen coupled cluster approach for the polyoxygen species. The results do not override the ones published previously (see Supporting Information for the detailed discussion and Table 1S). However, we employ the data to justify the CCSD(T,*full*)/cc-pCVTZ and CCSD(T,FC)/aug-cc-pVTZ theory levels chosen here for the main computational study.

Calculated vs Experimental Data. In the presented study, we use the corresponding physicochemical data to verify and justify the high-correlated methods and basis sets applied to the oxygen species. Despite the single reference wave functions used for the description of singlet states of O and O_2, the calculated energies and spectral characteristics of the first excited singlet states of atomic and molecular oxygen as well as the geometric parameter (bond length) for O_2 show that these states correspond to the multiconfigurational wave functions of $O(^1D)$ and $O_2(a^1\Delta_g)$ states, which are triple and double degenerate, respectively, not to $O(^1S)$ and $O_2(b^1\Sigma_g^+)$, as takes place frequently in many single-reference calculations. This is probably due to the effect of CCSD(T) excitations ,which take into account the large part of the nondynamic correlation required to form the multiconfigurational states. At the same time, the wave function remains to be a proper CCSD(T) solution, as is evident from the values of T_1-diagnosis (<0.02). As is evident from Table 1S (see Supporting Information), the agreement between the calculated and experimental energies of singlet−triplet transitions of O and O_2 species for $O(^1D) \leftarrow O(^3P)$ and $O_2(a^1\Delta_g) \leftarrow O_2(X^3\Sigma_g^-)$ transitions was typically in the range of 15% (10−15 kJ mol^{-1}) at all the theoretical levels and was in better agreement than for $O_2(b^1\Sigma_g^+) \leftarrow O_2(X^3\Sigma_g^-)$ (error about 100%). Geometry parameters and vibrational frequencies are also satisfactorily represented for O_2 both in triplet and singlet electronic states. Typical deviation of the calculated harmonic vibrational frequencies is about 10 cm^{-1} for the $O_2(^3\Sigma_g^-)$ vibrations and 40−50 cm^{-1} for the $O_2(^1\Delta_g)$ vibrations. The latest discrepancy has probably some contribution due to the lower accuracy of experimental data on the excited $O_2(^1\Delta_g)$ state.

The vibrational frequencies of O_3 (719.6, 1062.1, 1157.8 cm^{-1}) and O_2 (1580.19 cm^{-1} for $^3\Sigma_g^-$ electronic state) calculated at the CCSD(T,*full*)/cc-pCVTZ level are in good agreement with the experimental harmonic frequencies 716.0 cm^{-1}, 1089.2 cm^{-1}, 1134.9 cm^{-1}, and 1589.15 cm^{-1} for the O_3 $(\tilde{X}^1A_1)$ open form[80] and $O_2(^3\Sigma_g^-)$,[81] respectively. It should also be noted that the data calculated at the CCSD(T,full)/cc-pCVTZ level are in agreement with CCSD(T,full)/cc-pVTZ and CCSD(T)/aug-cc-pVTZ results. However, inclusion of a tight core function in the basis set improves significantly the calculated data for O_2 and O_3. At the CCSD(T,*full*)/cc-pCVTZ level, the differences from the experimental parameters for O_2 ($^3\Sigma_g^-$ and $^1\Delta_g$) and $O_3(\tilde{X}^1A_1)$ are only about 0.001 Å for O−O bond lengths and about 25 cm^{-1} for the "worst case" of vibrational frequency ν_3 (symmetric stretch belonging to $^1A_1$ irreducible representation) of ozone, which is well-known to be difficult to correctly predict.[59,82−88]

Watts and Bartlett[86] performed a very extensive survey of coupled cluster methodology up to the CCSDT method. On this basis, we calculated the remaining error from the neglect of relativity and made a direct comparison with experimental data. We calculated the average internuclear distances (r_g) and the distance between the average nuclear positions (r_a) with a harmonic force field and cubic force constants calculated at the CCSD(T,FC)/aug-cc-pVQZ theory level. The errors were found to be negligibly small. Details of this analysis are given in the Supporting Information.

Previously, Müller et al.[89] explored the PES of the O_3 system using the multireference configuration interaction (MR-CI) method in both internally contracted (ic) and non-contracted

variants, as well as the multireference coupled cluster (MR-AQCC) method and CCSD(T) values for the O_3 optimization. Later, Holka et al.[90] obtained an excellent agreement with experimental values at the icMR-CISD and icMR-AQCC theory levels (for a discussion of the results, see Supporting Information). This improvement is considered a success of the multireference methodology.[91,92] However, single reference methods have a significant advantage[93] because they have more satisfactory scaling of computational time at a similar quality of results. This evolution of implementations and competition among two groups of methods are reviewed in detail in refs 91, 92, and 94.

The Cyclic O_3 (D_{3h}) Molecule. The existence of the cyclic (D_{3h}) ozone isomer as a metastable structure was proposed by Peyerimhoff and Buenker[95] on the basis of HF-SCF calculations and was confirmed later using post-HF methods.[96−100] The results of the coupled cluster calculations at the CCSD(T)/NASA-Ames-ANO theory level confirmed[101] this conclusion. It was also supported by PES exploration with the CASSCF method.[102] The origin of the metastability of cyclic O_3 was analyzed by multireference calculations in refs 103−105 and by the rate constant calculations for the reaction $O_3(D_{3h}) \rightarrow O_2 + O$ in ref 106.

We calculated the parameters for the D_{3h} form of O_3 at the CCSD(T,full)/cc-pCVTZ level (see Table 1S). The calculated structural and energetic parameters are in good agreement with the characteristics of this stationary point obtained earlier at other levels of theory[89,106−108] including CCSD(T)/aug-cc-pV5Z and the CBS-Q model of Peterson, MRCI, and MR-AQCC with full valence active space CAS(18,12) in conjunction cc-pCV5Z and aug,cc-pV5Z basis sets.

Performance of the Single Reference Coupled Cluster Theory for O, O_2, and O_3: Focal Point Analysis. The agreement between the calculated and experimental energies of singlet−triplet transitions of O and O_2 species for $O(^1D) \leftarrow O(^3P)$ and $O_2(a^1\Delta_g) \leftarrow O_2(X^3\Sigma_g^-)$ transitions was in good agreement with experimental data. However, the observed performance can be caused by a fortuitous compensation of errors for the high-correlated system at the CCSD(T) theory levels. A similar situation can be anticipated for the gap between $O_3(D_{3h})$ and $O_3(C_{2v})$. The focal point analysis[72−74] was carried out in the present study for O and O_2 (the latter was optimized at the CCSDT(fc)/cc-pVTZ level) with energy calculation up to CCSDTQ(fc)/cc-pVTZ and for O_3 (both optimized at the CCSD(T,*full*)/aug-cc-pCVTZ level) with energy calculation up to CCSDT(Q). The data are collected in Table 3S. The total energies for $O(^3P)$ and $O_2(^3\Sigma_g^-)$ calculated here are in agreement with those obtained earlier.[109] A small difference in energies for $O_2(^3\Sigma_g^-)$ is very likely to be from a small difference in the molecular geometries. For $O(^1D) \leftarrow O(^3P)$ and $O_2(a^1\Delta_g) \leftarrow O_2(X^3\Sigma_g^-)$ transitions, the values near the full coupled cluster limit are as follows: 196.66 and 99.52 kJ mol^{-1} at CCSDTQ(fc)/cc-pVTZ, where the estimated errors are not more than 1.08 and 0.28 kJ mol^{-1}. The CCSDT(Q) data are in excellent agreement with the results of the full iterative CCSDTQ approach. The CCSD(T) values (213.63 and 125.4 kJ mol^{-1}) are a reasonably good estimate for the calculated property. For the O atom, the convergence of the coupled cluster expansion is smooth, whereas for the O_2 system the inclusion of quadruple excitations using perturbation theory increased the increment up to a value of 15.05 kJ mol^{-1}, which is higher than the value of the (CCSDT-CCSD(T)) increment. However, after the full iterative treatment by the CCSDTQ method, the result did not change significantly. This observation makes it possible to conclude that the error for the gap (126.35 kJ mol^{-1}) calculated at the CCSDT(Q)/cc-pVTZ level should be lower than the corresponding increment value (6.92 kJ mol^{-1}).

The data given in Table 2S justify the ability of the CCSD(T) method to reproduce properly the main features of oxygen-rich species and reliability of the calculated values (geometrical parameters and harmonic vibrational frequencies) for other species under investigation. Among all the results obtained here, the ones obtained at the CCSD(T,full)/cc-pCVTZ level demonstrate the best agreement for both geometry and vibrational parameters of these molecules among all the CCSD(T) calculations within correlation consistent VTZ-basis sets (Table 1S). We conclude that the combination of the CCSD(T) method with the basis extended by the core functions with explicitly involved core orbitals in the correlated calculations is the most prominent model for the modeling of polyoxygen substances.

Tetraoxygen. For the O_4 molecule, both isomers reported earlier were located on the singlet PES: cyclic D_{2d} (see Figure 1a) and open (star-like) D_{3h} (Figure 1b). On the triplet PES,

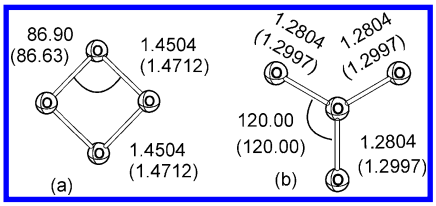

Figure 1. The structures of cyclic O_4 (a) and star-like O_4 (b) optimized at the CCSD(FC)/cc-pVTZ and CCSD(T)/cc-pCVTZ (in parentheses) levels. Bond lengths are given in Å, bond angles in degrees.

the O_4 molecule does not exist. It was noticed previously[9] that the cyclic isomer of the O_4 molecule has mainly single reference character of the wave function.

It was supposed earlier on the basis of CAS(6,6), CAS(8,8), and CAS(16,12) calculations[20] that the O_4 system could be described correctly in the CAS(24,16) active space. To our knowledge, such a kind of theory has not been applied to O_4 molecules up to date because it is considered impractical.[20]

In the present study, we performed the local minima search for both *cyc*-O_4 and *acycl*-O_4 at the CAS(24,16)/cc-pVDZ theory level (i.e., full valence active space for the given system) without any symmetry and geometrical constraints followed by the harmonic frequencies calculation. The *cyc*-O_4 and *acycl*-O_4 isomers converged to structures characterized by D_{2d} and D_{3h} point groups correspondingly (see Figure 1). The vibrational frequency analysis confirmed that both the stationary points are true local minima. Molecule O_4 (D_{3h}) is more energetically favorable, and the energy of the isomerization reaction O_4 (D_{2d}) → O_4 (D_{3h}) is 89.3 kJ mol^{-1}.

The CI vector of the CASSCF(24,16) wave function consists of 1 657 110 CSFs. The analysis of the configuration interaction (CI) amplitudes for CASSCF(24,16)/cc-pVDZ obtained for both O_4 (D_{3h}) and O_4 (D_{2d}) structures shows that the relative weight of the Hartree−Fock configurations (the squared first coefficient of CI expansion vector) is about 0.8. On the basis of this fact and the fact that the structural and energetic parameters calculated at the CCSD(T) and CAS(24,16) levels are close to each other, we conclude that the errors of a single-

reference CCSD(T) approximation do not influence the results significantly.

For the star-like O_4 structure, the CASSCF calculations with extending active spaces up to CAS(16,12) within 6-31G(d), cc-pVDZ, ANO-DZ, and 6-311G(d) basis sets result in a symmetry breaking structure with a C_{2v} point group that is usually explained by the influence of intruder states.[9] All the attempts to extend the active space by including corresponding quasi-degenerate virtual orbitals and truncate the (24,16) active space by excluding corresponding quasi-degenerate occupied orbitals failed, and no symmetric structures were found.

The low-symmetry chain-like O_4 structure (Figure 2) is a local minimum at the CCSD/cc-pVTZ level. A similar structure

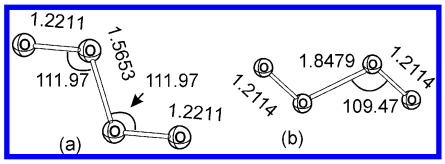

Figure 2. The structures of singlet chain-like O_4 (a) and triplet chain-like O_4 (b) optimized at the CCSD(FC)/cc-pVTZ. Bond lengths are given in Å, bond angles in degrees.

was reported earlier.[110] The geometry optimization results in the C_{2h} (zig-zag) structure with an energy of 88.5 kJ mol^{-1} relative to $O_2(^3\Sigma_g^-)$. The structure (Figure 2) remains a local minimum also in the triplet state (with a somewhat elongated intermolecular distance: r(O···O) = 1.8481 Å). However, at higher levels of theory (CCSD(T)/cc-pCVDZ and CCSD(T)/cc-pCVTZ), this structure (both in singlet and triplet states) rearranges to the structures of O_2···O_2 (D_2) or O_3···O (C_1) complexes. The latest one undergoes further rearrangements, as will be described below.

Additional efforts to localize O_4 chain-like structures were applied using a search of local minima at the singlet and triplet PESs of the system at the CAS(16,12)/cc-pVDZ and CAS(24,16)/cc-pVDZ levels. The optimization runs started from a set of structures belong to two point groups C_{2v}, C_2 (planar zig-zag), and C_2 (screw-like). All structures dissociated to the O_2···O_2 complexes (D_{2d} symmetry group), and no one structure corresponded to the O_4 chain molecule.

Energies, geometry parameters, vibrational frequencies, and IR intensities for both cyclic (D_{2d}) and open (D_{3h}) structures calculated at the CCSD(T) level are given in Table 2 and Table 2S. Like the CASSCF calculations, the cyclic structure O_4 (D_{2d}) is significantly more favorable (by 81.3 kJ mol^{-1}) in energy than the star-like O_4 (D_{3h}) isomer. Surprisingly, this value is very close to the energy of 89.3 kJ mol^{-1} calculated at the CAS(24,16)/cc-pVDZ level. To the best of out knowledge, no high-correlated quantum chemical comparative studies were performed for both O_4 isomers. From earlier studies of these molecules,[5,9] it can be deduced that the predicted gap between O_4 (D_{2d}) and O_4 (D_{3h}) is within a few electronvolts. In a more recent study,[26] it was calculated to be 1.22 eV at the CCSD(T)/TZ2P theory level. However, in the present study, we found the correct active space to describe both O_4 molecules. Thus, it made it possible to carry out the energy refinements using MRCI methods in the CAS(24,16) active space. The energies of the isomerization reaction O_4 (D_{2d}) → O_4 (D_{3h}) calculated at the MRCI+Q/cc-pVTZ and MRCI-DDCI-3/cc-pVTZ theory levels for the structures optimized at the CCSD(T,*full*)/cc-pCVTZ are 70.2 and 73.4 kJ mol^{-1}, respectively. Both values are in reasonably good agreement with this one (89.3 kJ mol^{-1}) obtained at the CCSD(T,*full*)/cc-pCVTZ level. Thus, CCSD(T,*full*)/cc-pCVTZ was verified at the basis of multi-reference calculations. For the $O_2(a^1\Delta_g)$←$O_2(X^3\Sigma_g^-)$ transition, the MRCI+Q/cc-pVTZ and MRCI-DDCI-3/cc-pVTZ data (101.2 and 97.8 kJ mol^{-1} or 101.6 and 98.4 mol^{-1} calculated with CAS(8,6) or CAS(12,8) active spaces, respectively) are in excellent agreement with CCSDT-(Q) and CCSDTQ computational results (99.2 and 99.5 kJ mol^{-1}).

Energies of some hypothetical reactions of the O_4 isomers' production calculated at the CCSD(T)/cc-pCVTZ and CCSDT(Q)/cc-pVTZ (in parentheses) levels and using MRCI+Q/cc-pVTZ//CCSD(T)/cc-pCVTZ and MRCI-DDCI-3/cc-pVTZ//CCSD(T)/cc-pCVTZ composite approaches (in brackets) are

$$O_2(^3\Sigma_g^-) + O_2(^3\Sigma_g^-) \rightarrow O_4(^1A,\ D_{3h})$$

$$\Delta_r E = 480.0\ (466.3)\ \text{kJ mol}^{-1}\ \text{and}\ 490.9\ [483.3]\ \text{kJ mol}^{-1}$$

$$O_2(^3\Sigma_g^-) + O_2(^3\Sigma_g^-) \rightarrow O_4(^1A,\ D_{2d})$$

$$\Delta_r E = 398.7\ (396.4)\ \text{kJ mol}^{-1}\ \text{and}\ 420.6\ [409.9]\ \text{kJ mol}^{-1}$$

$$O_2(^1\Delta_g) + O_2(^1\Delta_g) \rightarrow O_4(^1A,\ D_{3h})$$

$$\Delta_r E = 229.3\ (267.8)\ \text{kJ mol}^{-1}\ \text{and}\ 287.6\ [286.5]\ \text{kJ mol}^{-1}$$

$$O_2(^1\Delta_g) + O_2(^1\Delta_g) \rightarrow O_4(^1A,\ D_{2d})$$

$$\Delta_r E = 148.0\ (197.5)\ \text{kJ mol}^{-1}\ \text{and}\ 215.4\ [213.1]\ \text{kJ mol}^{-1}$$

$$O(^1D) + O_3(^1A_1) \rightarrow O_4(^1A,\ D_{3h})$$

$$\Delta_r E = -134.3\ (-120.1)\ \text{kJ mol}^{-1}$$

$$O(^1D) + O_3(^1A_1) \rightarrow O_4(^1A,\ D_{2d})$$

$$\Delta_r E = -215.7\ (-189.9)\ \text{kJ mol}^{-1}$$

Both O_4 isomers are much higher in energy than molecular oxygen in both the triplet and singlet states. The quasi-isolated $O_2(^3\Sigma_g^-)$ + $O_2(^3\Sigma_g^-)$ monomers were calculated at distances of 10 and 12 Å. In two sets of calculations, the differences between energies of the system at 10 and 12 Å were about 3.7 and 3.2 kJ mol^{-1} for the MRCI+Q and MRCI-DDCI-3 methods, respectively, revealing the approximate size consistency. The $O_2(^3\Sigma_g^-)$ + $O_2(^3\Sigma_g^-)$ → $O_4(^1A, D_{2d})$ reaction energy calculated at the MRCI+Q and MRCI-DDCI-3 levels based on CAS-(16,12) active space are 416.3 and 489.9 kJ mol^{-1}, respectevely, with the estimated errors resulting from the incomplete optimization of about 5.7 and 3.2 kJ mol^{-1}. We also obtained significant disagreement in E_r for the $O_2(^3\Sigma_g^-)$ + $O_2(^3\Sigma_g^-)$ → $O_4(^1A, D_{2d})$ reaction calculated with MRCI-DDCI-3 in the active space (16,12) in comparison with those obtained with MRCI-DDCI-3 based on the CAS(24,16)/cc-pVTZ wave function and with MRCI+Q based on CAS(16,12) and CAS(24,16) as well as with the CCSD(T) and CCSDT(Q) methods. This significant discrepancy is not due to a lack of important configurations. This is justified by calculations with reduced selection criteria (T_{pre} and T_{sel}) to 10^{-7} and 10^{-9} au (the resulting E_r value is changed by 1.6 kJ mol^{-1}). This is likely aroused from an imbalanced treatment of electron correlation

dx.doi.org/10.1021/ct3006584 | J. Chem. Theory Comput. 2013, 9, 247−262

by simplified MR-DDCI-3 wave functions in the truncated model CAS(16,12) active space with respect to MRCI+Q. Hence, we conclude that the MRCI+Q/cc-pVTZ theory level provides a reliable estimate for the E_r in both active spaces, whereas the MR-DDCI-3 method is valid only in the largest active space CAS(24,16).

The E_r values for MRCI methods and obtained at the CCSDT(Q)/cc-pVTZ theory level for *cyc*-O_4 production in both $O_2 + O_2$ and $O_3 + O$ channels are in good agreement with the data calculated previously in ref 22 with the FN-QMC method on the CAS(16,12)SCF wave function; in ref 17 with the CCSD(T), CASPT2 (RS2), and MR-ACPF methods in conjunction with aug-cc-pVQZ basis set; and in refs 7 and 16 at the CAS(16,12)SCF/ANO-DZ and CISD/DZP theory levels. The calculated values for all the formation reaction energies and the $O_4(D_{2d})-O_4(D_{3h})$ gap are in strong disagreement with those reported in ref 26: the $O_4(D_{2d})$ and $O_4(D_{3h})$ formation energies and the gap between O_4 isomers are as follows: 511.4, 629.1, and 117.7 kJ mol^{-1}. The employed[26] TZ2P basis set with an (11s6p3d)/[5s3p2d] contraction scheme is not enough since it does not provide converged results.

Performance of the Single Reference Coupled Cluster Theory for O_4 (D_{3h}) and O_4 (D_{2d}): Focal Point Analysis. To verify the reliability of the CCSD(T) results for the O_4 (D_{2d})−O_4 (D_{3h}) gap calculation, we performed the focal point analysis in the set of calculations up to CCSDT(Q)/cc-pVTZ (Table 4S). The CCSD(T) and CCSDT data (80.7 kJ mol^{-1} and 80.3 kJ mol^{-1}, respectively) are in excellent agreement between each other; i.e., the corresponding increment is only 0.5 kJ mol^{-1}, and in the both MRCI calculated values. The inclusion of the quadruple disconnected clusters decreased the energy gap to 69.9 kJ mol^{-1}, while the increment is 10.4 kJ mol^{-1} for the CCSDT(Q)-CCSDT pair. The excellent agreement of the CCSDT(Q)/cc-pVTZ results with those obtained by the MRCI and MRCI-DDCI-3 calculations is very likely to be elucidated by the significant influence of non-dynamic electron correlation, which is only partially covered by the CCSD(T) method, since the nonmonotonous convergence for the coupled cluster expansion (Table 4S) was observed for an energetic difference between the O_4 isomers. However, the CCSD(T) method is still competing in comparison with the most advanced CCSDT(Q) and multireference approaches.

Pentaoxygen. The cyclic conformation of the O_5 molecule (C_s, open nonplanar envelope) was found at the CCSD (CCSD/cc-pVDZ and CCSD/cc-pVTZ, see Table 1 and Table 2S) and CASSCF (CAS(20,15) and CAS(10,10) in conjunction with cc-pVDZ and cc-pVTZ basis sets) levels in the singlet state $^1A'$. On the triplet PES, the cyclic O_5 structure was not located. The optimized geometry is shown in Figure 3. It should be noted that the value of 0.026 for the T_1 diagnostic of CCSD shows a remarkable influence of nondynamic electron correlation not completely covered by single and double excitations.

The CAS(20,15)/cc-pVTZ calculation gives a cyclic structure very similar to that obtained at the CCSD/cc-pVTZ level. This C_s structure (nonplanar open envelope) has O···O bond distances of 1.454 Å and valence angles O···O−O of about 100° (see Figure 3).

To examine the importance of static electron correlation corresponding to the quasi−degenerate orbitals, we performed the stationary point search with the CASSCF method in different active spaces. It was possible to decrease the active space to (10,10) without the intruder states problem in O_5 geometry optimization. The structure for the active space (10,10) is characterized by the C_s point group (see Figure 3) and has considerably different bond lengths in comparison with CAS(20,15)/cc-pVTZ (the O_1-O_2 bond length 1.433 Å and 1.417 for (10,10) and (20,15) active spaces, respectively, and the O_3-O_4 bond length from 1.538 to 1.505 Å). The O_2-O_3 bond length was not affected by the choice of active space (1.454 and 1.457 Å). The relative weights of the Hartree−Fock configurations are about 0.79 and 0.82 for the CAS(20,15) and CAS(10,10) active spaces, respectively.

It is hard to accurately estimate the dissociation energy at the CASSCF level because it is not rigorously size-consistent in the truncated active space. At the CAS(20,15)/cc-pVDZ level, it was possible to find the saddle point for homolytic dissociation $O_5 \rightarrow O_3 + O_2$ at the CAS(20,15)/cc-pVDZ level in the geometry optimization without any constraints (Figure 4).

The transition state is characterized by the C_s point group and the relative weight of the Hartree−Fock configuration by about 0.75. The comparison between the structures of local minimum and transition state shows that the O−O bond length corresponding to eliminated dioxygen $O_2(^1\Delta_g)$ is significantly reduced in TS by about 0.15 Å (from 1.586 Å to 1.435 Å) in contrast with the O−O bond length corresponding to the forming ozone molecule which is only moderately reduced by 0.071 Å (from 1.436 Å to 1.365 Å). The O···O distance between O_2 and O_3 fragments is increased by about 0.22 Å.

Table 1. Calculated Energies and Geometry Parameters of the Covalently Bound Forms of O_5 and O_6 Polymorphs (Vibrational Frequencies and Intensities Given in Supporting Information)[a]

theory level	ΔE,[b] kJ mol^{-1}	geometry
	O_5 (singlet C_s, cyclic)	
CCSD/cc-pVTZ	77.2 (rel.O_3 + $O_2(^1\Delta_g)$)	Figure 3
CCSD(T,full)/cc-pCVTZ	dissociation to $O_3\cdots O_2$ (van der Waals complex)	
	O_6 (singlet D_{3d}, chair)	
CCSD/cc-pVTZ	67.4	1.4122 Å, 38.1°
CCSD(T,full)/cc-pCVTZ	58.3	1.4294 Å, 103.6°
	O_6 (singlet D_{2d}, twist)	
CCSD/cc-pVTZ	78.2	1.4491 Å, 1.3698 Å, 104.1°, 105.1°
CCSD(T,full)/cc-pCVTZ	dissociation with O−O bond cleavage	

[a]For the O_4 data, see Supporting Information. [b]Energy of O_n per atom relative to $(1/2)O_2(^3\Sigma_g)$.

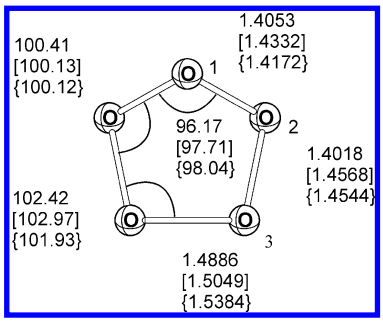

Figure 3. The structure of O_5 optimized at the CCSD(FC)/cc-pVTZ, CAS(10,10)/cc-pVTZ [in square brackets], and CAS(20,15)/cc-pVTZ {in curly brackets} theory levels. Bond lengths are given in Å, bond angles in degrees.

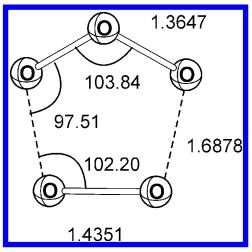

Figure 4. The structure of the saddle point for O_5 dissociation ($O_5 \rightarrow O_3 + O_2$) optimized at the CAS(20,15)/cc-pVDZ theory level. Bond lengths are given in Å, bond angles in degrees.

The activation energy E_a of the synchronous dissociation is 8.6 kJ mol^{-1} at the CAS(20,15)/cc-pVDZ level; the energy of the reaction $O_5(^1A') \rightarrow O_3(^1A_1) + O_2(^1\Delta_g)$ is −41.1 kJ mol^{-1}. This shows that CASSCF in the truncated active space underestimates the energy of the reaction probably because of noneffective treatment of the dynamical electron correlation.

At the CCSD(T,*full*)/cc-pCVTZ level (Table 1), all the attempts to find the covalently bound structure for the O_5 molecule failed despite many different starting structures being used. Geometry optimization at this level proceeds via the longest (1.53 Å) O−O bond cleavage and finishes near floppy complex OO···O···OO with the unconverged CCSD procedure, which is evident for the obvious multireference character of the complex. The T_1-diagnostic value 0.0268 calculated at the CCSD/cc-pVDZ level at the structure corresponding to the CAS(20,15)/cc-pVDZ local minimum was noticeably higher than 0.02.

The contradiction between CASSCF and CCSD(T) approaches deserves a special consideration. The main shortcoming of the CCSD(T) method is the loss of accuracy in the presence of electronic orbitals' near degeneracies. However, it is not obvious whether the near degeneracy can cause the failure of the single reference approach in any particular case, e.g., in cyclic O_5 because sometimes singlet biradicals (well-known bad-behaved systems) can be described correctly at the CCSD(T) level.[111] Many tests were proposed to analyze this necessity: the T_1 diagnostic,[112,113] its alternative D_1 diagnostic, examination of the largest T_2 amplitude,[114] and other methods reviewed in ref 115 (see also refs 116 and 117 and references therein).

In our study, the T_1 diagnostic and the largest T_2 amplitude calculated at the CCSD(fc)/cc-pVDZ theory level at the structure corresponding to the CAS(20,15)/cc-pVTZ local minimum were 0.026 and 0.0728, respectively. Both values and weights of Hartree−Fock configurations indicate that static electron correlation is not negligible; however, the effect is not strongly pronounced. At the same time, the CASSCF calculations have a lack of electron correlation within the CASSCF wave function and have completely no correlation within the core orbitals. The core orbital correlation has a significant effect on the electronic energy. To expose an artifact of CASSCF or CCSD(T) methods for the prediction of O_5 molecular structure existence, a stationary point search without any constraint at the full-electron RI-NEVPT2/cc-pVTZ//cc-pVTZ/C theory level with the CAS(10,10) active space with two increments for numerical differentiation (0.005 au and 0.001 au) was performed. For all the optimizations, O−O bond cleavage was observed, although the convergence to any complex was not reached since the active space (10,10) is not size-consistent. The geometry optimization with the approximate size-consistent (20,15) active space is prohibitively time-demanding. Thus, it is believed that the CCSD(T) results are more reliable than both CCSD and CASSCF methods, and there is no bound structure for the O_5 complexes except probably extremely weak van der Waals long-distance contact. The cyclic O_5 molecule is an artifact of CCSD or CASSCF calculations due to the lack of dynamic electron correlation taken into account.

Hexaoxygen. For the covalently bound O_6 molecule, the closed structure of the six-membered nonplanar cycle can exist, in principle, in three conformations: D_{3d} ("chair"), D_{2d} ("twist"), and C_{2v} ("boat"). Among them, only two (D_{3d} and D_{2d}) were located at the CCSD/cc-pVTZ level (Figure 5).

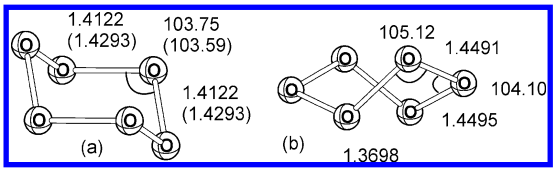

Figure 5. The structures of the "chair" conformer O_6 (a) and "twist" conformer O_6 (b) optimized at the CCSD(FC)/cc-pVTZ and CCSD(T,*full*)/cc-pCVTZ (in parentheses) theory levels. Bond lengths are given in Å, bond angles in degrees.

However, at the higher CCSD(T,*full*)/cc-pCVTZ theory level, only the D_{3d} conformation was located (Table 1 and Table 2S). Other conformations were rearranging to the different structures (typically to O_2 molecules) during the optimization. The D_{3d} conformation is only one structure, being the subject of previous quantum chemical investigations.[18,43] However, the CCSD(T,*full*)/cc-pCVTZ level used in the present study is the highest level of theory ever achieved for this substance.

Harmonic frequencies and the corresponding IR intensities calculated at the CCSD(T,*full*)/cc-pCVTZ level are also presented in Table 2 and Table 2S. It is seen that the covalent bonding results in quite significant changes of the vibrational frequencies. Thus, the spectral features of these molecules isolated in the low-temperature matrices cannot be observed in the region of spectral bands of source O_3.

The value of the T_1 diagnostic calculated at the CCSD/cc-pVTZ level for corresponding local minima is 0.023, which demonstrates that the nondynamic electron correlation is probably mostly covered by the CCSD(T) method. The CCSD(T) method reproduces correctly also the symmetry and degeneracy of vibration modes for the D_{3d} structures (see Table 2 and Table 2S).

The most surprising property of the located hexaoxygen structure is its quite low relative energy regarding the energy of two separate ozone molecules. The relative energy of the D_{3d} conformation is only 58 kJ mol^{-1} higher relative to free ozone molecules. The low dimerization energy takes place at both the CCSD and CCSD(T) levels. Similar results are obtained also for thermodynamic properties of the compounds calculated in harmonic approximation. The low energy of the O_6 (D_{3d}) molecule relative to free ozone raises the question of the possibility of experimental observation or synthesis of this structure. On the basis of common physicochemical rules, we can predict that this molecule can be formed from ozone under high pressure conditions.

We carried out the full geometry optimizations at the CAS(16,14)/STO-3G level for both conformers. For the "chair" conformer localized at the CCSD(T)/cc-pCVTZ

dx.doi.org/10.1021/ct3006584 | J. Chem. Theory Comput. 2013, 9, 247−262

Table 2. Calculated Energies and Geometry Parameters for the Atomic-Molecular van der Waals Complexes of O_n (n = 3 and 4)

theory level	E_b,[a] kJ mol^{-1}	geometry (bond lengths in Å, angles in degrees)
	O_2···O (quintet) $C_{\infty v}$	
CCSD/cc-pVTZ	−0.54 (rel. $O_2(^3\Sigma_g^-)$ + $O(^3P)$)	r(O−O) = 1.2013 Å, r(O···O) = 3.2682 Å
CCSD(T)/aug-cc-pVTZ	−1.49 (rel. $O_2(^3\Sigma_g^-)$ + $O(^3P)$)	r(O−O) = 1.2131 Å, r(O···O) = 2.9768 Å
CCSD(T,full)/cc-pCVTZ	−0.87 (rel. $O_2(^3\Sigma_g^-)$ + $O(^3P)$)	r(O−O) = 1.2098 Å, r(O···O) = 3.1097 Å
	O_2···O (triplet)	
CCSD/cc-pVTZ	−184.6 (rel. $O_2(^3\Sigma_g^-)$ + $O(^1D)$)	r(O−O) = 1.2020 Å, r(O···O) = 3.1759 Å
	−89.8 (rel. $O_2(^1\Delta_g)$ + $O(^3P)$)	α(O−O···O) = 180°
	48.1 (rel. $O_2(^3\Sigma_g^-)$ + $O(^3P)$)	
CCSD(T)/aug-cc-pVTZ	−67.0 (rel. $O_2(^3\Sigma_g^-)$ + $O(^1D)$)	r(O−O) = 1.2129 Å, r(O···O) = 3.5310 Å
	−77.7 (rel. $O_2(^1\Delta_g)$ + $O(^3P)$)	α(O−O···O) = 80.11°
	46.8 (rel. $O_2(^3\Sigma_g^-)$ + $O(^3P)$)	
CCSD(T,full)/cc-pCVTZ	−166.6 (rel. $O_2(^3\Sigma_g^-)$ + $O(^1D)$)	r(O−O) = 1.2098 Å, r(O···O) = 3.1610 Å
	−76.9 (rel. $O_2(^1\Delta_g)$ + $O(^3P)$)	α(O−O···O) = 180°
	48.4 (rel. $O_2(^3\Sigma_g^-)$ + $O(^3P)$)	
	O_2···O (singlet)	
activationless rearrangement to O_3 (finished with unconverged CCSD)		
	O_3···O (singlet)	
CCSD/cc-pVTZ	*b*	*b*
CCSD(T)/aug-cc-pVTZ	−3.6 (rel. $O_3(^1A_1)$ + $O(^1D)$)	see Figure 7
CCSD(T,full)/cc-pCVTZ	−3.1 (rel. $O_3(^1A_1)$ + $O(^1D)$)	see Figure 7
	O_3···O (triplet)	
CCSD/cc-pVTZ	−1.5 (rel. $O_3(^1A_1)$ + $O(^3P)$)	see Figure 8a
CCSD(T)/aug-cc-pVTZ	−5.2 (rel. $O_3(^1A_1)$ + $O(^3P)$)	see Figure 8b
CCSD(T)/aug-cc-pVTZ	−0.9 (rel. $O_3(^1A_1)$ + $O(^3P)$)	see Figure 8c

[a]Binding energy of the complex relatively to the separate monomers. [b]Structure does not exist at this theory level.

level, the corresponding stationary point was also found at the CAS(16,14)/STO-3G level, and the performed frequency analysis showed that the located structure is a true local minimum (see Figure 6). The "boat" and "twist" conformers do not exist at this theory level, rearranging to the broken symmetry structures, which is probably explained by the intruder states effects.

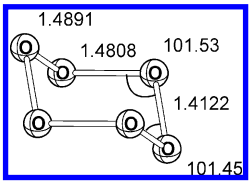

Figure 6. The structure of the "chair" conformer O_6 optimized at the CAS(16,14)/STO-3G theory level. Bond lengths are given in Å, bond angles in degrees.

The CI vector of the CAS(16,14)/STO-3G wave function gives a weight of the Hartree−Fock configuration of about 0.748. This value supports the conclusion about the necessity of inclusion of triple excitations in the coupled-cluster ansatz for qualitative prediction of vibrational spectra. Expanding of the basis set to 6-31G(d) and cc-pVDZ produced distorted molecular structures.

Active space CAS(16,14) for O_6 does not converge correctly to dissociation limit $O_6 \rightarrow 2O_3$. We suppose that the full valence active space CAS(24,18) is enough to describe the reaction path because it includes all (quasi)degenerate orbitals, and active space CAS(12,9) shows correct results for the ozone molecule. However, it was impossible to perform the CAS(24,18) calculations for O_6 even with conjunction of the STO-3G basis set because of prohibitive time demands for the active space including 172 320 330 CSFs. Unfortunately, we failed to find any transition state of the dissociation channels. In all the runs, the optimization collapsed to completely erroneous structures with O−O bonds lower than 0.5 Å. This was probably because of the internal instability of the CCSD(T) procedure with many near-degenerate electronic states.

O_2···O Complex. The full optimization of the O_2···O complex in the quintet state ($O_2(^3\Sigma_g$)···O(^{3}P)) at the CCSD(T)/aug-cc-pVTZ and CCSD(T,*full*)/cc-pCVTZ levels results in a linear structure ($C_{\infty v}$ point group) with binding energies of 1.49 and 0.87 kJ mol^{-1} (124 and 64 cm^{-1}, Table 2), respectively. These values are in good agreement with the previous MRCI+D/aug-cc-pVQZ calculation for the quintet O_3 PES cuts along fixed geometry points.[118,119] The value found there was about 100 cm^{-1}, although the structures were not collinear.

It should be specially noted that the optimization of O_2···O is successful only after a thorough preliminary search of suitable starting orbital occupations, which was performed with the OCCUPATION keyword in the CFOUR suite of programs. The standard orbital occupations based on the Aufbau principle results in no CCSD convergence. As a rule, the same situation takes place also for other weak complexes described below.

In the triplet state, the optimized structures at the CCSD/cc-pVTZ and CCSD(T,*full*)/cc-pCVTZ levels have significantly higher absolute energies than for the quintet state. It seems that the CCSD procedure converges to the metastable excited states of the O_3 molecule with an energy of about 48 kJ mol^{-1} relative to the source $O_2(^3\Sigma_g^-)$ + $O(^3P)$ system. All the attempts to optimize the O_2···O complex in the singlet state at the CCSD and CCSD(T) levels failed. During the optimization, the activationless rearrangement to the O_3 molecule was occurring, which typically finished with the unconverged CCSD procedure. In both quintet and triplet spin states, the complex has only a typical oxygen band near 1600 cm^{-1}, only slightly distorted by the intermolecular interaction. No new bands in the region of 1000−1200 cm^{-1} which are typical for the free or distorted ozone molecule in the ground state were observed.

For all the local minima optimized for the O_2···O complex, the zero-point vibration energy calculated in harmonic approximation is much higher than the binding energy of the complex (typically about 10 kJ mol^{-1} for ZPE in comparison with 0.5−1.5 kJ mol^{-1} for E_b (Table 2)). Thus, even accounting for the approximate character of the ZPE estimation, it is quite doubtful that the complex can exist as a structurally stable compound.

O_3···O Complex. The question of the existence of the complex between ozone and the ground state of the atomic

oxygen O(^{3}P) arose as a possible explanation of the experimental results obtained in the experiments on the UV (210−250 nm) irradiation of solid oxygen at temperatures of 10−30 K. Initially, Schriver-Mazuolli et al.[52] found that UV irradiation with a xenon lamp results in the formation of low-intensity features at 1033 and 1036 cm^{-1} near the ν_3 band of ozone. Later, Dyer et al.[53] reported the formation of a strong stable band structure after irradiation of the solid oxygen with a UV laser at 210−260 nm. The new series of intense bands (comparable to the very intense ν_3 band of ozone) were observed in region 1029−1038 cm^{-1}. In both cases, the new bands were stable over rather long time intervals and slowly disappeared during annealing to 30 K. The new bands were interpreted as a formation of the complex $O_3\cdots O(^3P)$. These results were then repeated at a slower resolution to describe the ozone formation from the solid oxygen in the cosmic space.[120,121] In both experimental works, the shoulders of the ozone ν_3 low-frequency band wings were registered after irradiation. The wings were stable over several minutes after irradiation and were interpreted as a formation of the $O_3\cdots O$ complex.

At the same time, the calculations of the O(^{3}P) + O_3 PES performed at the CAS(16,12) + CASMP2/ANO-TZ level did not show any remarkable minimum corresponding to this complex [16] at the S_0, T_0, and T_1 PESs (first two correspond to $O_2(X^3\Sigma_g^-)$ + $O_2(X^3\Sigma_g^-)$ and the third one corresponds to $O_2(X^3\Sigma_g^-)$ + $O_2(^1\Delta_g)$ asymptotic). Later Varandas and Llanio-Trujillo,[20] in the CASSCF and MRCI calculations with different active spaces for the CASSCF reference wave function of the O_3 + O system at the triplet (^{3}A) PES, found two TSs for the O_3 + O → O_2 + O_2 reaction with the CASSCF(8,8) method, with an additional intermediate between them. However, the geometry of the intermediate was not reported. This local minimum disappeared at the CAS(8,8)-MRCI/6-311(2d,f) level at the same basis set (with single remaining TS). Thus, controversies exist concerning the existence of the $O_3\cdots O$ complex at the triplet PES of the ozone−atomic oxygen PES. It should also be noted that a similar situation takes place for the existence of the complex $O_2\cdots O$ at the PES calculated at very comprehensive levels of theory.[122,123] The comparison of the kinetic constants was calculated using very accurate PESs (which have a local minimum corresponding to the $O_2\cdots O$ complex) does imperfectly agree with the available experimental data, whereas the artificial removal of the local minimum from the PES gives perfect agreement with experimental values.[103,119]

In order to elucidate the existence of the complex, we performed a study of the $O_3\cdots O$ system at different levels of CCSD(T) theory in different spin states. As before, a thorough search of suitable starting occupations was performed before the optimization. While the search of correct electron population was performed (see Table 6S for the determined OCCUPATION values), it was taken into account that the intermolecular distances in the complex are quite long (3.2−3.7 Å). It is believed that the interaction has mostly van der Waals character, and the interaction of O(^{3}P) and O(^{1}D) atoms with ozone molecules should be approximately equal in energy. At first, the full optimizations were performed at the CAS(16,12)/cc-pVDZ and CAS(24,16)/cc-pVDZ levels for different structures of the $O_3\cdots O$ complex in singlet and triplet spin states (see Table 2 and Table 6S). Next for the symmetrical structures we retained the found point groups in the coupled cluster calculations.

The singlet state complexes ($O_2O\cdots O$ and $OO_2\cdots O$) were additionally optimized with lower geometry restrictions to obtain the planar and nonplanar structures of C_s symmetry at the CCSD(T)/cc-pCVTZ and CCSD(T)/aug-cc-pVTZ theory levels. Among the nonplanar singlet structures, the C_s conformation was located at both the CCSD(T)/aug-cc-pVTZ and CCSD(T,*full*)cc-pCVTZ levels (Figure 7). However, the first one has an imaginary frequency (98*i* cm^{-1}), and the second one has a frequency of 1811 cm^{-1}, which is obviously an artifact that arose because of Hessian instability. Thus, the stability (Table 2) of this structure is questionable.

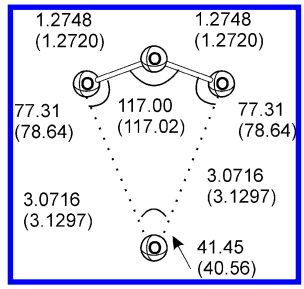

Figure 7. The structure of the $O_3\cdots O$ complex in singlet spin state optimized with constraints (C_s point group) at the CCSD(T,FC)/aug-cc-pVTZ and CCSD(T,*full*)/cc-pCVTZ (in brackets) theory levels. Bond lengths are given in Å, bond angles in degrees.

After the symmetry and geometry restrictions were completely eliminated, the optimization of the complex rearranged quickly to the asymmetric O−O−O···O structure and then started to rearrange to two oxygen molecules (singlet state). Simultaneously, the CCSD(T) wave function quickly collapsed to an improper solution with a high value of the largest T_2 amplitude of 0.06−0.09, and then the calculations were usually breaking due to the bad convergence of CCSD. This rearrangement is in agreement with the CAS(16,12)/cc-pVDZ optimization.

In the triplet state, three different C_s local minima distinguished by arrangement of the ozone O atoms bounded to O were found at the CCSD/cc-pVTZ (Figure 8a) and CCSD(T)/aug-cc-pVTZ levels (Figure 8b,c). At the CCSD-(T)/aug-cc-pVTZ theory level, the most stable conformation is the quasi-cyclic nonplanar structure with the O atom bonded to two terminal atoms of ozone. The binding energy (Table 2) of this conformation is valuable (5.2 kJ mol^{-1}) in comparison with the thermal energy at the solid oxygen temperatures (kT = 0.4 kJ mol^{-1}); however, it is significantly less than the harmonic ZPE value for this structure (18.2 kJ mol^{-1}). The second structure (Figure 8c) is much less favorable; its binding energy is only 0.9 kJ mol^{-1}. In this conformation, the O atom is bound to the central atom of ozone. It should be noted that the frequencies calculated at the same level of theory result in an IR shift of the ozone ν_3 frequency of −53 cm^{-1} for the first structure and +48 cm^{-1} for the second one. Thus, the shifted ν_3 bands do not correspond to any experimentally registered features. However, such large IR shifts in the case of the extremely weakly bound complex cause concern that the results can be affected by the Hessian instability due to the influence of the numerous almost-degenerate orbitals or because artificial permutations of orbitals performed to achieve the convergence of the CCSD procedure.

On the basis of these results, we conclude that the $O_3\cdots O$ complex has a quite instable character. At the best level of

dx.doi.org/10.1021/ct3006584 | J. Chem. Theory Comput. 2013, 9, 247−262

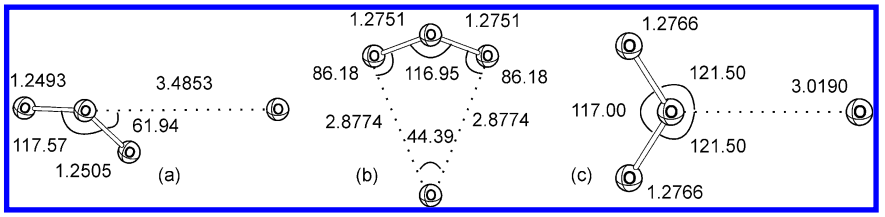

Figure 8. The structures of the $O_3\cdots O$ complex in the triplet spin state optimized at the CCSD(FC)/cc-pVTZ (a, full optimization), CCSD(T,FC)/aug-cc-pVTZ (b, constraint C_s point group) and (c, constraint C_{2v} point group) theory levels. Bond lengths are given in Å, bond angles in degrees.

theory, the binding energy is much less than the ZPE energy. At the same time, the energies of reactions with the formation of two dioxygens estimated at the CCSD(T)/cc-pCVTZ and CCSDT(Q,fc)/cc-pVTZ levels are

$$O_3 + O(^1D) \rightarrow 2O_2(^1\Delta_g)$$

$$(-360.7 \text{ and } -387.9 \text{ kJ mol}^{-1})$$

$$O_3 + O(^3P) \rightarrow 2O_2(^3\Sigma_g^-)$$

$$(-397.5 \text{ and } -388.6 \text{ kJ mol}^{-1})$$

The CASSCF method does not treat efficiently the dynamic electron correlation in the restricted model active space, which is possible to employ for this system. Thus, the binding energy will be significantly overestimated. However, the main properties of the solutions (structures and symmetry point group) can be investigated in order to verify the CCSD(T) results or to guide the subsequent time-demanding geometry optimization with the CCSD(T) method. All the structures depicted in Figure 8 were located on the singlet and triplet PESs in the CAS(16,12)/cc-pVDZ calculations. Hence, while the CCSD-(T) optimizations converged, the calculated results are verified and can be used for the determination of the $O_3\cdots O$ complexes' production and comparison of theoretical and experimental IR shifts. While the structure obtained with the CASSCF calculation does not exist in a stationary point search with CCSD(T)/cc-pCVTZ and especially CCSD(T)/aug-cc-pVTZ (more reliable for van der Waals complexes localization), it is very likely to be a result of insufficient treatment of the dynamic electron correlation and therefore an artificial localization of the complex.

As was demonstrated by the calculations, the first reaction has low activation energy (the optimization tended to two O_2 fragments as described above). There are no serious doubts that the second reaction which is also spin-allowed with higher reaction energy has no remarkable barrier of rearrangement. Thus, such a complex cannot stay stable during the long interval of time and should quickly disappear after even slight annealing. Thus, in our opinion, the assignment made on the basis of UV irradiation experiments in refs 52, 53, 120, and 121 should be considered with caution. In our opinion, the possible causes of the intense bands in the 1037−1029 cm^{-1} region after irradiation could be a result of the formation of ozone monomer molecules or ozone dimers in the matrix environment strongly distorted by the photochemical reactions of oxygen dissociation.

There are also some additional indirect arguments supporting this point of view. First of all, as was described above, the high-level calculations of the $O_2\cdots O$ triplet PES give the local minimum for the $O_2\cdots O$ complex (probably metastable, i.e., with the TS of rearrangement to O_3 lying lower than the energy of isolated reagents), which has a binding energy of about 200 cm^{-1} (0.6 kcal/mol) and an activation barrier of dissociation in the range of 0−200 cm^{-1}. Thus, the activation energy of removal of $O(^3P)$ in the solid oxygen matrix (in an environment where $O_2\cdots O$ contacts are abundant) cannot be significantly higher even if the $O(^3P)$ atom forms complexes with O_3.

Anyway, to our knowledge, the structure and the properties of $O_3\cdots O$ reported here are a first consideration of this complex performed at the theoretical level providing qualitative correspondence between the calculated and observed properties of ozone and its van der Waals complexes.

Oxygen Dimer. There are abundant studies about the existence of (O_2) dimers, both experimental[33,124,125] and theoretical (see, e.g., review book chapter[126]) because of the significance of these systems for the chemistry of the atmosphere[127] and chemical lasers.[128,129]

Dioxygen dimers $(O_2)_2$ still remain a great challenge for quantum chemistry because of an intermolecular type of bonding and different spin couplings which require multireference and high correlated wave functions for quantum chemical description of the electronic structure. For descriptions of the energies and spectral characteristics of all the conformations, the good approximations were applied for both ground and excited states in ref 130 where the CASPT2 method with active space CAS(16,12) in conjunction with the ANO-TZ basis set and the inclusion of a spin−orbital interaction by means of the CAS(12,8) active space and ANO-DZ basis set; in ref 131 where SA-CAS(4,4)PT2 and SA-CAS(4,4)SCF with van der Waals correction by *ab initio* results; and in ref 132 where CASPT2, MRCI, ACPF, and composite CCSD(T)/MRCI approaches were applied. The most extensive survey of different electronic states is ref 133. However, it was performed at a moderate theory level CAS(4,4)CI/6-311G(d) and only for the H-shaped conformer. Recently, the potential energy curves for all of the proposed conformers of the dimer in 13 electronic states were revised in refs 34 and 40.

In contrast to singlet and triplet spin states, the quintet spin state of the complex $(O_2)_2$ can be described by high-correlated *ab initio* methods which are the most reliable and exceed significantly the CASPT2 approach for the treatment of intermolecular interactions in weakly bound systems if nondynamical electron correlation is not significant. The PES of the O_2 dimer was explored with energy calculation using the CCSD(T) method with systematic extension of the ANO−TZ basis set [132] and with the aug-cc-pVQZ basis set and extended manifold of the grid points to reconstruct the PES.[134]

It was reported earlier, that the oxygen dimer exists in several conformations (T-shaped, X-shaped, linear, and cyclic) and different spin states. However, it was found in the present study that the rectangular conformation is unlikely. All the attempts to optimize it at the CCSD(T) levels resulted either in twisting

to the twisted (partly X-shaped) D_{2d} conformation or in the rhomboid D_2 structure. If the rectangular structure was achieved, it typically had imaginary vibrational modes tending to twist the conformation. The only local minima for the rectangular conformation (both triplet and singlet) were found at the CCSD/cc-pVTZ levels. The obtained results show that the oxygen dimers in the quintet state form weak van der Waals complexes with typical binding energies of about 1.3−1.7 kJ mol^{-1}, which is in good agreement with the experimental estimates 1.65 ± 0.08 kJ mol^{-1} in ref 124. The similar values of the binding energy take place in the case of the triplet spin state. The energies and vibrational frequencies of all the located conformations of the O_2 dimer are given in Table 3 and Table 5S; the structures are shown in Figure 9.

The calculation shows that the frequencies of all the conformations are typically slightly distorted frequencies of dioxygen molecules, as expected for the weak molecular complexes. Thus, it is impossible that the dioxygen dimers' vibrations contribute in any remarkable way to the infrared shifts observed due to oxygen irradiation (observed in the region of ozone bands).

Complex $O_3\cdots O_2$. In contrast with the structures discussed above, the complex $O_3\cdots O_2$ was not described earlier, and it is considered for the first time. However, its vibrational frequencies should be close to the observed O_3 frequencies because of small perturbation of the $O_3(^1A_1)$ molecule by the singlet ($^1\Delta_g$) and triplet ($^3\Sigma_g^-$) dioxygen.

The CAS(20,15)/cc-pVDZ theory level was chosen for a preliminary search because of the proven size-consistency of this active space, which corresponds to the CAS(12,9) active space for active O_3 and CAS(8,6) for O_2. Five different structures were examined as the starting points. The optimized structures are characterized by the C_s point group in singlet ($^1A'$) and triplet ($^3A'$) spin states and are shown in Figure 10. For $O_3\cdots O_2$ ($^1A'$), the Hartree−Fock configuration is not leading ,whereas for the $O_3\cdots O_2$ ($^3A'$) its weight is about 0.77. Thus, the probable significant influence of the nondynamic correlation effect can be anticipated from the CASSCF calculations for both spin states of the quasi-cyclic $O_3\cdots O_2$ complex (see Table 4).

Optimized at the CAS(20,15)/cc-pVDZ level, quasi-cyclic structures were initially for optimizations at different levels with energy calculations using the coupled cluster method. For the singlet ($^1A'$) state, the quasi-cyclic stationary points were located at the CCSD(T)/cc-pCVTZ and CCSD(T)/aug-cc-pVTZ levels (Figure 10). However, by harmonic vibrational frequency analysis it was not confirmed that the C_s-symmetric van der Waals complex of ozone and dioxygen corresponds to local minima. In this case, there is a small C_s symmetry breaking imaginary frequency (26.8*i* and 42.6*i* cm^{-1}) at the CCSD(T)/cc-pCVTZ and CCSD(T)/aug-cc-pVTZ levels of theory. This imaginary mode corresponds to the twisting of dioxygen relative to ozone. However, during the reoptimization along this symmetry-breaking mode, no asymmetrical conformations were located because the optimization restored the symmetrical structure.

The calculated shifts of ν_1, ν_2, and ν_3 for the O_3 fragment are 1.2, −3.7, and 0.6 and 0.9, −6.6, and 0.2 cm^{-1} for CCSD(T)/cc-pCVTZ and CCSD(T)/aug-cc-pVTZ, respectively.

The probable influence of non-dynamical electron correlation of O_2 ($^1\Delta_g$) determined by a T_1 diagnostic value of 0.023 and artificial (non-physical) convergence of the HF-SCF solution for the $O_3\cdots O_2$ complex in the triplet spin state

Table 3. Calculated Energies and Geometry Parameters for the Intermolecular van der Waals Complexes of O_n (n = 4)

theory level	E_b,[a] kJ mol^{-1}	geometry (bond lengths in Å, angles in degrees)
	$(O_2)_2$ (quintet D_{2d}, twisted)	
CCSD/cc-pVTZ	−1.3 (rel. $2O_2(^3\Sigma_g^-)$)	r(O−O) = 1.2010 Å, r(O···O) = 3.4102 Å
		α(O−O···O) = 79.75°, θ(O−O···O−O) = 88.79°
CCSD(T)/aug-cc-pVTZ	−2.1 (rel. $2O_2(^3\Sigma_g^-)$)	r(O−O) = 1.2132 Å, r(O···O) = 3.3211Å
		α(O−O···O) = 78.95°, θ(O−O···O−O) = 90.2°
CCSD(T,full)/cc-pCVTZ	−1.6 (rel. $2O_2(^3\Sigma_g^-)$)	r(O−O) = 1.2100 Å, r(O···O) = 3.3545 Å
		α(O−O···O) = 79.6°, θ(O−O..O−O) = 88.1°
	$(O_2)_2$ (quintet D_{2h}, optimization started from rectangular conformation)	
CCSD/cc-pVTZ	−1.3 (rel. $2O_2(^3\Sigma_g^-)$)	(C_{2h} approximately D_{2h}, parallelogram)
		r(O−O) = 1.2010 Å, r(O···O) = 3.4457 Å
		α(O−O···O) = 71.5°
CCSD(T,full)/cc-pCVTZ	−1.4 (rel. $2O_2(^3\Sigma_g^-)$)	r(O−O) = 1.2101 Å, r(O···O) = 3.3806Å
CCSD(T,full)/cc-pCVTZ[b]	−1.6 (rel. $2O_2(^3\Sigma_g^-)$)	r(O−O) = 1.2086 Å, r(O···O) = 3.3885 Å
		α(O−O···O) = 72.3 °
	$(O_2)_2$ (triplet D_{2d}, twisted, X-shaped)	
CCSD/cc-pVTZ	129.5 (rel. $O_2(^3\Sigma_g^-)$ and $O_2(^1\Delta_g)$)	r(O−O) = 1.1951 Å, r(O···O) = 2.7068Å
		α(O−O···O) = 77.2°, θ(O−O..O−O) = 87.1°
	$(O_2)_2$ (singlet D_{2d}, twisted, X-shaped)	
CCSD/cc-pVTZ	[c]	[c]
CCSD(T,full)/cc-pCVTZ	−0.1 (rel. $O_2(^1\Delta_g)$)	r(O−O) = 1.2235 Å, r(O···O) = 3.5825 Å
		α(O−O···O) = 80.2°, θ(O−O···O−O) = 88.3°
	$(O_2)_2$ (singlet D_{2h}, rectangle)	
CCSD/cc-pVTZ	−1.71 (rel. $O_2(^1\Delta_g)$)	r(O−O) = 1.1942 Å, r(O···O) = 1.8944 Å
CCSD(T,full)/cc-pCVTZ	[c]	[c]
	$(O_2)_2$ (triplet D_{2h}, rectangle)	
CCSD/cc-pVTZ	18.12 (rel. $O_2(^3\Sigma_g^-)$ and $O_2(^1\Delta_g)$)	r(O−O) = 1.1973 Å, r(O···O) = 2.0997 Å
CCSD(T,full)/cc-pCVTZ	[c]	[c]

[a]Binding energy of the complex relatively to the separate monomers. [b]Constraint dihedral angle 180°. [c]Structure does not exist at this theory level.

which resulted in the lack of correlation with separated O_2 ($^3\Sigma_g^-$) and $O_3(^1A_1)$ caused, for the first case, symmetry breaking of the complex $O_3\cdots O_2$ ($^1A'$) characterized by the C_s point group optimized at the CAS(20,15)/cc-pVDZ level and, for the second case, an impossibility of localizing the intermolecular complex $O_3\cdots O_2$, which exists obviously from a physical point of view that was confirmed rigorously at the CAS(20,15)/cc-pVDZ theory level.

Ozone Dimer $(O_3)_2$. The optimization of the molecular complex of ozone on the CCSD(T)/aug-cc-pVTZ and CCSD(T)/cc-pCVTZ levels results in two structures corresponding to the van der Waals dimer. The first conformation is an open structure of C_s symmetry. This corresponds completely to the structure found earlier by Slanina and Adamowicz[51] (T-

dx.doi.org/10.1021/ct3006584 | J. Chem. Theory Comput. 2013, 9, 247−262

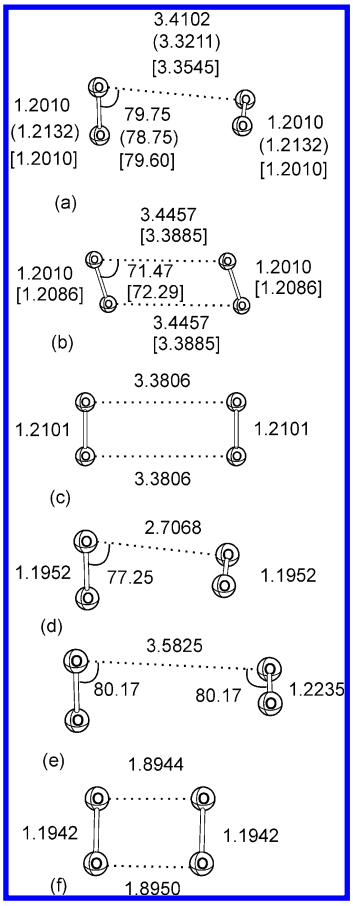

Figure 9. The structures of the complexes $(O_2)_2$, D_{2d} (a), $(O_2)_2$, C_{2h} (b), $(O_2)_2$, D_{2h} (c) in the quintet spin state; $(O_2)_2$ and D_{2d} (d) in the triplet spin; and $(O_2)_2$, D_{2d} (e), $(O_2)_2$, and D_{2h} (f) in the singlet spin state optimized at the CCSD(FC)/cc-pVTZ, CCSD(T,FC)/aug-cc-pVTZ (in parentheses) and CCSD(T,full)/cc-pCVTZ [in square brackets] theory levels. Bond lengths are given in Å, bond angles in degrees.

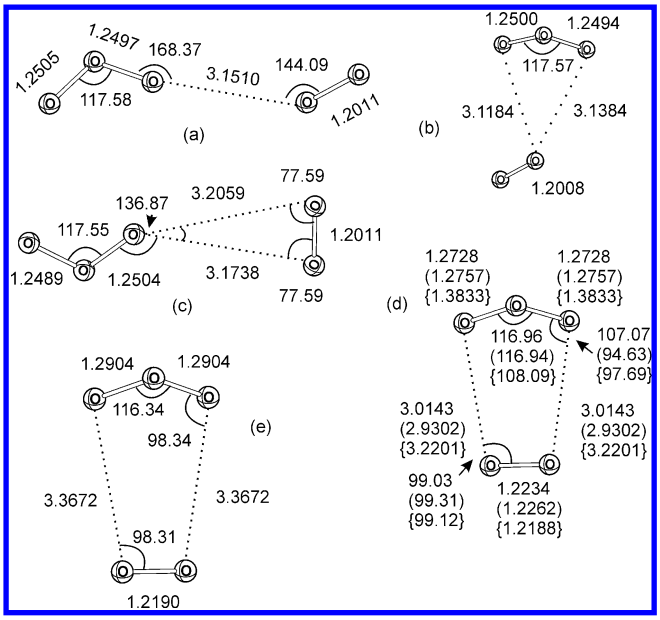

Figure 10. The structures of the complexes $O_3\cdots O_2$ (a and b) in the triplet spin state and $O_3\cdots O_2$ in the singlet spin state optimized (c) at the CCSD(FC)/cc-pVTZ theory level and (d) at the CAS(20,15)/cc-pVDZ, CCSD(T,*full*)/cc-pCVTZ (in parentheses) and CCSD(T,FC)/aug-cc-pVTZ {in curly brackets} theory levels. The structure of the complex $O_3\cdots O_2$ (e) in the triplet spin state optimized at the CAS(20,15)/cc-pVDZ theory level. Bond lengths are given in Å, bond angles in degrees.

shaped conformation). The geometry of the complex is shown in Figure 11. The energy of the conformation is about 8.0 kJ mol^{-1} at the CCSD(T)/cc-pCVTZ level (7.1 kJ mol^{-1} at CCSD(T)/aug-cc-pVTZ, see Table 4).

Another located conformation is the closed (six-membered quasi-cyclic) structure of C_{2h} symmetry with two O···O contacts of 2.8 Å. Up to date, there were no reports on the structure of this shape. At the CCSD(T) level of theory, this structure is more stable than the T-shaped conformation both in the cc-pCVTZ and aug-cc-pVTZ bases, the calculated binding energies are 8.4 and 9.2 kJ mol^{-1}, respectively.

The harmonic frequencies of the T-shaped conformation calculated at the CCSD(T)/cc-pCVTZ level show that the complex is characterized by two positive infrared shifts of the ω_3 harmonic frequency of ozone: +2 and +4 cm^{-1}. Earlier,[135] it was reported that the ozone dimer in argon, nitrogen, and oxygen matrices is characterized by two doublets close to the ν_3 ozone band, which were interpreted as the bands of ozone dimer in two different matrix sites with shifts of about +2 and −4 cm^{-1}. However, on the basis of the present results, it seems that another assignment is more suitable—two different sites with the positive (+2, +4) and negative (−2, −4) shifts.

The calculation of the IR frequencies for the quasi-cyclic conformation gives two bands near the ν_2 ozone band. The IR shifts of these bands are (IR intensities in km mol^{-1} are given in parentheses) −28.2 (0) and 16.9(182) cm^{-1} at CCSD(T,*full*)/cc-pCVTZ and −34.1(0) and 17.9(210) cm^{-1} at CCSD(T,FC)/aug-cc-pVTZ. However, only one of these bands with positive IR shifts has significant IR intensity.

On the basis of these data, we conclude that the only possible assignment for the experimentally observed bands is the T-shaped conformation in the two different sites of the low-temperature matrix. Although the quasi-cyclic structure is somewhat more favorable in the gas phase, it is unfavorable in the matrix probably because the structure of this conformation is not suitable for the structure of the matrix environment.

CONCLUSIONS

In the current work, we performed a comparative study for the structures, energies, and (if applicable) vibrational frequencies of the species O_n (n = 1−6) with emphasis on the structural, energetic, and IR-spectral properties of the molecules which can be potentially formed during the irradiation of solid oxygen by UV and electron beams and can give the IR bands in the region of ozone ν_3 vibration. The goal was to elucidate the question of whether it is possible to explain the observed spectral features in the region of the ozone IR band that arose after irradiation on the basis of higher oxygen allotropes or molecular complexes. Because of the different composition of the species, we used the CCSD(T,*full*)/cc-pCVTZ and CCSD(T,FC)/aug-cc-pVTZ levels of theory, instead of multi-reference CI or CCSD approaches, which are not practical for the full geometry optimizations, conformational analysis, and IR-spectra simulation in the case of n > 4. However, the chosen theory levels are verified by the focal point analysis method with energy calculations up to CCSDTQ(fc)/cc-pVTZ for O(^{1}D), O(^{3}P), O_2 ($^1\Delta_g$), and O_2 ($^3\Sigma_g^-$) and up to CCSDT-

dx.doi.org/10.1021/ct3006584 | J. Chem. Theory Comput. 2013, 9, 247−262

Table 4. Calculated Energies and Geometry Parameters for the van der Waals Complexes of O_n (n = 5 and 6)

theory level	E_b,[a] kJ mol^{-1}	geometry (bond lengths in Å, angles in degrees)
	$O_3\cdots O_2$ (triplet C_s, chain)	
CCSD/cc-pVTZ	−1.1(rel. $O_2(^3\Sigma_g^-)$ + O_3)	see Figure 10a
CCSD/cc-pVTZ	−0.7 (rel. $O_2(^3\Sigma_g^-)$ + O_3)	see Figure 10b
CCSD(T,full)/cc-pCVTZ	[c]	[c]
CAS(20,15)/cc-pVDZ	[c]	[c]
	$O_3\cdots O_2$ (singlet C_s, chain)	
CCSD/cc-pVTZ	−2.2 (rel. $O_2(^1\Delta_g)$ + O_3)	see Figure 10c
CCSD(T,full)/cc-pCVTZ	[c]	[c]
	$O_3\cdots O_2$ (singlet C_s, cyclic)	
CCSD(T,full)/cc-pCVTZ	−4.4 (rel. $O_2(^1\Delta_g)$ + O_3)	see Figure 10d
CCSD(T)/aug-cc-pVTZ	−5.3 (rel. $O_2(^1\Delta_g)$ + O_3)	see Figure 10d
CAS(20,15)/cc-pVDZ	[b]	see Figure 10d
	$O_3\cdots O_2$ (triplet C_s, cyclic)	
CAS(20,15)/cc-pVDZ	[b]	see Figure 10e
	$(O_3)_2$ (singlet C_s, T-shaped)	
CCSD/cc-pVTZ	−6.5 (rel. $2O_3$)	see Figure 11a
CCSD(T)/aug-cc-pVTZ	−7.9 (rel. $2O_3$)	see Figure 11a
CCSD(T,full)/cc-pCVTZ	−7.3 (rel. $2O_3$)	see Figure 11a
	$(O_3)_2$ (singlet C_i, quasi-cyclic)	
CCSD/cc-pVTZ	−6.8 (rel. $2O_3$)	see Figure 11b
CCSD(T)/aug-cc-pVTZ	−9.4 (rel. $2O_3$)	see Figure 11b
CCSD(T,full)/cc-pCVTZ	−8.3 (rel. $2O_3$)	see Figure 11b

[a]Binding energy of the complex relative to the separate monomers. [b]Overestimated at this theory level. [c]Structure does not exist at this theory level.

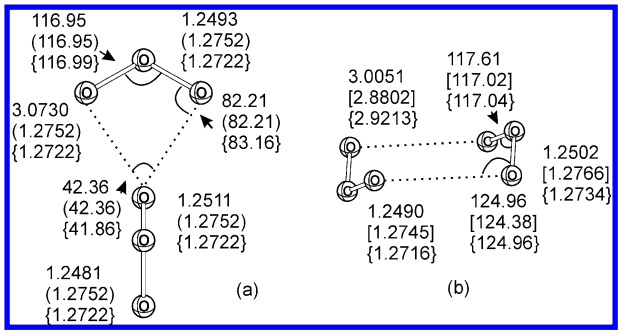

Figure 11. The structures of the complexes $O_3\cdots O_3$, C_s (a) and $O_3\cdots O_3$, C_i (b) optimized at the CCSD(FC)/cc-pVTZ, CCSD-(T,FC)/aug-cc-pVTZ (in parentheses), and CCSD(T,*full*)/cc-pCVTZ {in curly brackets} levels. Bond lengths are given in Å, bond angles in degrees.

(Q,fc)/cc-pVTZ for the O_3 isomers and the O_4 isomers. The provided best estimates for excitation energies for the cases $n \leq 2$ are in good agreement with the experimental one. The energetic gap $O_3(C_{2v}) \rightarrow O_3(D_{3h})$ obtained here with the CCSDT(Q) method is in excellent agreement with that previously calculated with the MRCI and MR-AQCC methods. For O_4 (D_{2d}) and O_4 (D_{3h}), formation and isomerization energies were calculated at the highest ever achieved level, CCSDT(Q)/cc-pVTZ. All the computational results for the single reference method were verified with the MRCI+Q and MRCI-DDCI-3 multireference methods in conjunction with cc-pVTZ basis set. The best estimates for the CCSDTQ and CCSDT(Q) are found to be in good agreement with the multireference data. On the basis of the overall comparison of experimental data and calculated results, we conclude that the CCSD(T) computational levels provide adequate results competing with the best obtained, whereas the most affordable CCSD/cc-pVTZ level is not a sufficiently highly correlated theory level for most of the studied systems.

Among the calculated structures, a new (cyclic) conformation was found for the $(O_3)_2$ complex. The local minima of the molecules O_4 and O_6 and the intermolecular complexes $(O_2)_2$, $(O_3)_2$, $O_2\cdots O_3$, and $O\cdots O_3$ in singlet and triplet states were studied for the first time using the CCSD and CCSD(T) quantum chemical methods up to the CCSD(T,*full*)/cc-pCVTZ and CCSD(T,FC)/aug-cc-pVTZ levels as well as at the CAS(16,12)/cc-pVDZ and CAS(24,16)/cc-pVDZ levels. The calculations demonstrate the existence of stable highly symmetric structures $O_4(D_{3h})$, $O_4(D_{2d})$, and O_6 (D_{3d}) in a singlet state as well as the complexes $O\cdots O_2$, $O_2\cdots O_3$, and $(O_3)_2$ in different conformations. Simultaneously, the existence of the complex $O_3\cdots O$ proposed earlier in the matrix isolation studies is not supported by the CCSD(T) calculations. The harmonic vibration frequencies of the ozone dimer for the located stationary points are in agreement with the IR spectra observed in the argon, solid nitrogen, and solid oxygen matrices. The CCSD(T) calculations performed here for the first time show that covalently bound O_5 in singlet and triplet spin states does not exist, which is in agreement with numerical optimization at the RI-NEVPT2/cc-pVTZ//cc-pVTZ/C level in active space (10,10). $O_3(D_{3h})$, O_4, and O_6 cannot give IR bands in the region of the ν_3 ozone bands (independently of the conformations), as well as the complex $O\cdots O_2$. The $O\cdots O_3$ complex in the singlet state does not exist at the CCSD(T)/cc-pCVTZ and CCSD(T,FC)/aug-cc-pVTZ levels, although the two conformations with binding energies of 5.4 and 0.9 kJ mol^{-1} were found for the triplet state. The frequencies of the located structures are poorly described within the CCSD(T) approach and require applications of more rigorous multireference methods. However, this structure cannot be so stable that it gives significant contributions to the long-living intense bands observed in solid oxygen. The most probable candidates for the assignments of the observed spectral features are the ozone dimeric complexes and/or monomeric ozone placed in a different environment (trapping sites) of the solid oxygen matrix. These results and recent experiments of Kulikov et al.[136] on the temperature dependence of the ν_3 ozone band show that the interpretation of the experiments given in refs 52 and 53 should be reconsidered. For the ozone dimer $(O_3)_2$, the second stable conformation found in the present work can potentially be registered in the gas phase and in the matrix.

■ ASSOCIATED CONTENT

Supporting Information

The total and relative energies, vibrational frequencies, Cartesian coordinates for the reported structures. This material is available free of charge via the Internet at http://pubs.acs.org

dx.doi.org/10.1021/ct3006584 | J. Chem. Theory Comput. 2013, 9, 247−262

AUTHOR INFORMATION

Corresponding Author

*E-mail: euriscomail@mail.ru (O.B.G.), ignatov@ichem.unn.ru (S.K.I.)

Author Contributions

⊥Authors contributed equally

Notes

The authors declare no competing financial interest.

ACKNOWLEDGMENTS

This work was supported by the Russian Foundation for Basic Research (projects No. 10-05-01112, 11-03-00085). OBG, SKI and MYK are thankful to DAAD and Alfred Wegener Institute for the fellowship support. O.B.G. is thankful to Kantharuban Sivalingam (Max−Planck Institute for Chemical Energy Conversion, Stiftstrasse 34-36, 45470 Mulheim an der Ruhr, Germany) for helpful discussion of specific features of multireference methods.

REFERENCES

(1) Dolezalek, Z. *Z. Phys. Chem.* **1910**, *71*, 191−213.
(2) Lewis, G. N. *J. Am. Chem. Soc.* **1924**, *46*, 2027−2032.
(3) Adamantides, V. *Chem. Phys.* **1980**, *48*, 221−225.
(4) Adamantides, V.; Neisius, D.; Verhaegen, G. *Chem. Phys.* **1980**, *48*, 215−220.
(5) Røeggen, I.; Nilssen, E. W. *Chem. Phys. Lett.* **1989**, *157*, 409−414.
(6) Feng, W. L.; Novaro, O. *Int. J. Quantum Chem.* **1984**, *26*, 521−533.
(7) Seidl, E. T.; Schaefer, H. F., III. *J. Chem. Phys.* **1988**, *88*, 7043−7049.
(8) Seidl, E. T.; Schaefer, H. F., III. *J. Chem. Phys.* **1992**, *96*, 1176−1182.
(9) Hotokka, M.; Pyykkö, P. *Chem. Phys. Lett.* **1989**, *157*, 415−418.
(10) Dunn, K. M.; Scuseria, G. E.; Schaefer, H. F., III. *J. Chem. Phys.* **1990**, *92*, 6077−6080.
(11) Ferreira, E.; Gardiol, P.; Sosa, R. M.; Ventura, O. N. *J. Mol. Struct.: THEOCHEM* **1995**, *335*, 63−68.
(12) Pavão, A. C.; Seabra, G. M.; Taft, C. A. *J. Mol. Struct.: THEOCHEM* **1995**, *335*, 59−61.
(13) Lauvergnat, D.; Clary, D. C. *J. Chem. Phys.* **1998**, *108*, 3566−3573.
(14) Gorelli, F. A.; Ulivi, L.; Santoro, M.; Bini, R. *Phys. Rev. Lett.* **1999**, *83*, 4093−4096.
(15) Hernández-Lamoneda, R.; Bartolomei, M.; Hernandez, M. I.; Campos-Martinez, J.; Dayou, F. *J. Phys. Chem. A* **2005**, *109*, 11587−11595.
(16) Hernández-Lamoneda, R.; Ramirez-Solis, A. *J. Chem. Phys.* **2000**, *113*, 4139−4145.
(17) Hernández-Lamoneda, R.; Ramirez-Solis, A. *J. Chem. Phys.* **2004**, *120*, 10084−10088.
(18) Politzer, P.; Lane, P. *Int. J. Quantum Chem.* **2000**, *77*, 336−340.
(19) Owens, F. J. *J. Mol. Struct.: THEOCHEM* **2001**, *546*, 261−264.
(20) Varandas, A. J. C.; Llanio-Trujillo, J. L. *Chem. Phys. Lett.* **2002**, *356*, 585−594.
(21) Pillay, D.; Wang, Y.; Hwang, G. S. *J. Am. Chem. Soc.* **2006**, *128*, 14000−14001.
(22) Caffarel, M.; Hernández-Lamoneda, R.; Scemama, A.; Ramírez-Solís, A. *Phys. Rev. Lett.* **2007**, *99*, 153001−153005.
(23) Ramírez-Solís, A.; Jolibois, F.; Maron, L. *Chem. Phys. Lett.* **2010**, *485*, 16−20.
(24) Goodarzi, M.; Piri, F.; Hajari, N.; Karimi, L. *Chem. Phys. Lett.* **2010**, *499*, 51−55.
(25) Caffarel, M.; Hernández-Lamoneda, R.; Scemama, A.; Ramírez-Solís, A. *Phys. Rev. Lett.* **2007**, *99*, 153001.
(26) Peterka, D. S.; Ahmed, M.; Suits, A. G.; Wilson, K. J.; Korkin, A.; Nooijen, M.; Bartlett, R. J. *J. Chem. Phys.* **1999**, *110*, 6095−6098.
(27) Peterka, D. S.; Ahmed, M.; Suits, A. G.; Wilson, K. J.; Korkin, A.; Nooijen, M.; Bartlett, R. J. *J. Chem. Phys.* **1999**, *111*, 5279−5279.
(28) Bevsek, H. M.; Ahmed, M.; Peterka, D. S.; Sailes, F. C.; Suits, A. G. *Faraday Discuss.* **1997**, *108*, 131−138.
(29) Chestakov, D. A.; Parker, D. H.; Dinu, L.; Baklanov, A. V. *J. Chem. Phys.* **2004**, *120*, 6794−6796.
(30) Cacace, F.; de Petris, G.; Troiani, A. *Angew. Chem., Int. Ed.* **2001**, *40*, 4062−4065.
(31) Long, C. A.; Ewing, G. E. *J. Chem. Phys.* **1973**, *58*, 4824−4834.
(32) Goodman, J.; Brus, L. E. *J. Chem. Phys.* **1977**, *67*, 4398−4407.
(33) Aquilanti, V.; Ascenzi, D.; Bartolomei, M.; Cappelletti, D.; Cavalli, S.; de Castro Vitores, M.; Pirani, F. *J. Am. Chem. Soc.* **1999**, *121*, 10794−10802.
(34) Nguyen, T.-N. V.; Timerghazin, Q. K.; Vach, H.; Peslherbe, G. H. *J. Chem. Phys.* **2011**, *134*, 064305−064312.
(35) Bartolomei, M.; Carmona-Novillo, E.; Hernández, M. I.; Pérez-Ríos, J.; Campos-Martínez, J.; Hernández-Lamoneda, R. *Phys. Rev. B* **2011**, *84*, 092105−092109.
(36) Hernández-Lamoneda, R.; Pérez-Ríos, J.; Carmona-Novillo, E.; Bartolomei, M.; Campos-Martínez, J.; Hernández, M. I. *Chem. Phys.* **2012**, *399*, 80−85.
(37) Ma, Y.; Oganov, A. R.; Glass, C. W. *Phys. Rev. B* **2007**, *76*, 064101.
(38) Meng, Y.; Eng, P. J.; Tse, J. S.; Shaw, D. M.; Hu, M. Y.; Shu, J.; Gramsch, S. A.; Kao, C.-c.; Hemley, R. J.; Mao, H. *Proc. Natl. Acad. Sci. U. S. A.* **2008**, *105*, 11640−11644.
(39) Daineka, D. V.; Pradere, F.; Chatelet, M.; Fort, E. *J. Appl. Phys.* **2002**, *92*, 1132−1136.
(40) Vach, H.; Nguyen, T.-N. V.; Timerghazin, Q. K.; Peslherbe, G. H. *Phys. Rev. Lett.* **2006**, *97*, 143402.
(41) Zhu, L.; Wang, Z.; Wang, Y.; Zou, G.; Mao, H.; Ma, Y. *Proc. Natl. Acad. Sci. U. S. A.* **2012**, *109*, 751−753.
(42) Blahous, C. P.; Schaefer, H. F., III. *J. Phys. Chem.* **1988**, *92*, 959−962.
(43) Xie, Y.; Schaefer, H. F., III; Jang, J. H.; Mhin, B. J.; Kim, H. S.; Yoon, C. W.; Kim, K. S. *Mol. Phys.* **1992**, *76*, 537−546.
(44) Zhao, M.; Gimarc, B. M. *J. Phys. Chem.* **1993**, *97*, 4023−4030.
(45) Gimarc, B. M.; Warren, D. S. *Croat. Chem. Acta* **1994**, *67*, 125−141.
(46) Gimarc, B. M.; Zhao, M. *J. Phys. Chem.* **1994**, *98*, 1596−1600.
(47) Gimarc, B. M.; Zhao, M. *Coord. Chem. Rev.* **1997**, *158*, 385−412.
(48) Probst, M.; Hermansson, K.; Urban, J.; Mach, P.; Muigg, D.; Denifl, G.; Fiegele, T.; Mason, N. J.; Stamatovic, A.; Mark, T. D. *J. Chem. Phys.* **2002**, *116*, 984−992.
(49) Murai, A.; Nakajima, T.; Tahara, N. *J. Comput. Chem., Jpn.* **2002**, *1*, 123−128.
(50) Slanina, Z. *Thermochim. Acta* **1990**, *173*, 171−176.
(51) Slanina, Z.; Adamowicz, L. *J. Atmos. Chem.* **1993**, *16*, 41−46.
(52) Schriver-Mazzuoli, L.; de Saxcé, A.; Lugez, C.; Camy-Peyret, C.; Schriver, A. *J. Chem. Phys.* **1995**, *102*, 690−701.
(53) Dyer, M. J.; Bressler, C. G.; Copeland, R. A. *Chem. Phys. Lett.* **1997**, *266*, 548−553.
(54) Sennikov, P. G.; Ignatov, S. K.; Schrems, O. *ChemPhysChem* **2005**, *6*, 392−412.
(55) Dunning, J. T. H. *J. Chem. Phys.* **1989**, *90*, 1007−1023.
(56) Woon, D. E.; Dunning, J. T. H. *J. Chem. Phys.* **1995**, *103*, 4572−4585.
(57) Bauschlicher, J. C. W.; Langhoff, S. R.; Taylor, P. R. *J. Chem. Phys.* **1988**, *88*, 2540−2546.
(58) Martin, J. M. L. *Chem. Phys. Lett.* **1995**, *242*, 343−350.
(59) Watts, J. D. Iterative and Non-Iterative Inclusion of Connected Triple Excitations in Coupled-Cluster Methods. Theory and Numerical Comparisons for Some Difficult Examples. In *Computational Chemistry: Reviews of Current Trends*; Leszczynski, J., Ed.; World Scientific: Singapore, 2002; Vol. *7*; pp 89−130.
(60) Frisch, M. J.; Trucks, G. W.; Schlegel, H. B.; Scuseria, G. E.; Robb, M. A.; Cheeseman, J. R.; Montgomery, J. A., Jr.; Vreven, T.; Kudin, K. N.; Burant, J. C.; Millam, J. M.; Iyengar, S. S.; Tomasi, J.; Barone, V.; Mennucci, B.; Cossi, M.; Scalmani, G.; Rega, N.;

Petersson, G. A.; Nakatsuji, H.; Hada, M.; Ehara, M.; Toyota, K.; Fukuda, R.; Hasegawa, J.; Ishida, M.; Nakajima, T.; Honda, Y.; Kitao, O.; Nakai, H.; Klene, M.; Li, X.; Knox, J. E.; Hratchian, H. P.; Cross, J. B.; Bakken, V.; Adamo, C.; Jaramillo, J.; Gomperts, R.; Stratmann, R. E.; Yazyev, O.; Austin, A. J.; Cammi, R.; Pomelli, C.; Ochterski, J. W.; Ayala, P. Y.; Morokuma, K.; Voth, G. A.; Salvador, P.; Dannenberg, J. J.; Zakrzewski, V. G.; Dapprich, S.; Daniels, A. D.; Strain, M. C.; Farkas, O.; Malick, D. K.; Rabuck, A. D.; Raghavachari, K.; Foresman, J. B.; Ortiz, J. V.; Cui, Q.; Baboul, A. G.; Clifford, S.; Cioslowski, J.; Stefanov, B. B.; Liu, G.; Liashenko, A.; Piskorz, P.; Komaromi, I.; Martin, R. L.; Fox, D. J.; Keith, T.; Al-Laham, M. A.; Peng, C. Y.; Nanayakkara, A.; Challacombe, M.; Gill, P. M. W.; Johnson, B.; Chen, W.; Wong, M. W.; Gonzalez, C.; Pople, J. A. *Gaussian 03*, version D.02; Gaussian, Inc.: Wallingford, CT, 2007.

(61) Granovsky, A. A. *Firefly*, version 7.1.G; Firefly Project: Moscow, Russia. http://classic.chem.msu.su/gran/firefly/index.html (accessed July 1, 2012).

(62) Schmidt, M. W.; Baldridge, K. K.; Boatz, J. A.; Elbert, S. T.; Gordon, M. S.; Jensen, J. H.; Koseki, S.; Matsunaga, N.; Nguyen, K. A.; Su, S. J.; Windus, T. L.; Dupuis, M.; Montgomery, J. A. *J. Comput. Chem.* **1993**, *14*, 1347−1363.

(63) Harding, M. E.; Metzroth, T.; Gauss, J.; Auer, A. A. *J. Chem. Theory Comput.* **2007**, *4*, 64−74.

(64) Stanton, J. F.; Gauss, J.; Harding, M. E.; Szalay, P. G.; Auer, A. A.; Bartlett, R. J.; Benedikt, U.; Berger, C.; Bernholdt, D. E.; Bomble, Y. J.; Cheng, L.; Christiansen, O.; Heckert, M.; Heun, O.; Huber, C.; Jagau, T.-C.; Jonsson, D.; Jusélius, J.; Klein, K.; Lauderdale, W. J.; Matthews, D. A.; Metzroth, T.; O'Neill, D. P.; Price, D. R.; Prochnow, E.; Ruud, K.; Schiffmann, F.; Schwalbach, W.; Stopkowicz, S.; Tajti, A.; Vazquez, J.; Wang, F.; Watts, J. D. *CFOUR*, version 1. Integral packages: Almlöf, J.; Taylor, P. R. *MOLECULE*; Taylor, P. R. *PROPS*; Helgaker, T.; Jensen, H. J. Aa.; Jørgensen, P.; Olsen, J. *ABACUS*; Mitin, A. V.; van Wüllen, C. *ECP*. http://www.cfour.de (accessed June 1, 2012).

(65) Scuseria, G. E. *J. Chem. Phys.* **1991**, *94*, 442−447.

(66) Watts, J. D.; Gauss, J.; Bartlett, R. J. *Chem. Phys. Lett.* **1992**, *200*, 1−7.

(67) Gauss, J.; Stanton, J. F. *Chem. Phys. Lett.* **1997**, *276*, 70−77.

(68) Szalay, P. G.; Gauss, J.; Stanton, J. F. *Theor. Chem. Acc.* **1998**, *100*, 5−11.

(69) Neese, F. *ORCA*, version 2.9.0; Max-Planck-Institute for Bioinorganic Chemistry: Ruhr, Germany, 2012.

(70) Kallay, M.; Surjan, P. R. *J. Chem. Phys.* **2001**, *115*, 2945−2954.

(71) Kállay, M. *MRCC*; TU Budapest: Budapest, Hungary. http://www.mrcc.hu (accessed October 1, 2012).

(72) Allen, W. D.; East, A. L. L.; Császár, A. G. Ab Initio Anharmonic Vibrational Analyses of Non-Rigid Molecules. In *Structures and Conformations of Nonrigid Molecules*; Laane, J., Dakkouri, M., van der Veken, B., Oberhammer, H., Eds.; Kluwer: Dordrecht, The Netherlands, 1993; pp 343−373.

(73) Csaszar, A. G.; Allen, W. D.; Schaefer, H. F., III. *J. Chem. Phys.* **1998**, *108*, 9751−9764.

(74) Schuurman, M. S.; Muir, S. R.; Allen, W. D.; Schaefer, H. F., III. *J. Chem. Phys.* **2004**, *120*, 11586−11599.

(75) Dennington, R.; Keith, T.; Millam, J. M.; Eppinnett, K.; Hovell, W. L.; Filliland, R. *GaussView*; Semichem, Inc.: Shawnee Mission, KS, 2009.

(76) Zhurko, G. *ChemCraft*, version 1.6 (build 348). http://www.chemcraftprog.com (accessed March 20, 2012)

(77) Ignatov, S. K. *MOLTRAN*, version 2.5; University of Nizhny Novgorod: Nizhny Novgorod, Russia, 2007. http://ichem.unn.ru/Moltran (accessed March 20, 2012).

(78) Kearns, D. R. *Chem. Rev.* **1971**, *71*, 395−427.

(79) Schweitzer, C.; Schmidt, R. *Chem. Rev.* **2003**, *103*, 1685−1758.

(80) Barbe, A.; Secroun, C.; Jouve, P. *J. Mol. Spectrosc.* **1974**, *49*, 171−182.

(81) Huber, K. P.; Herzberg, G. *Molecular Spectra and Molecular Structure. IV. Constants of Diatomic Molecules*; Van Nostrand: New York, 1979; Vol. *1*.

(82) Raghavachari, K.; Trucks, G. W.; Pople, J. A.; Replogle, E. *Chem. Phys. Lett.* **1989**, *158*, 207−212.

(83) Lee, T. J.; Scuseria, G. E. *J. Chem. Phys.* **1990**, *93*, 489−494.

(84) Leininger, M. L.; Schaefer, H. F., III. *J. Chem. Phys.* **1997**, *107*, 9059−9062.

(85) Hino, O.; Kinoshita, T.; Chan, G. K.-L.; Bartlett, R. J. *J. Chem. Phys.* **2006**, *124*, 114311−114317.

(86) Watts, J. D.; Bartlett, R. J. *J. Chem. Phys.* **1998**, *108*, 2511−2514.

(87) Stanton, J. F.; Lipscomb, W. N.; Magers, D. H.; Bartlett, R. J. *J. Chem. Phys.* **1989**, *90*, 1077−1082.

(88) Helgaker, T.; Gauss, J.; Jorgensen, P.; Olsen, J. *J. Chem. Phys.* **1997**, *106*, 6430−6440.

(89) Müller, T.; Xantheas, S. S.; Dachsel, H.; Harrison, R. J.; Nieplocha, J.; Shepard, R.; Kedziora, G. S.; Lischka, H. *Chem. Phys. Lett.* **1998**, *293*, 72−80.

(90) Holka, F.; Szalay, P. G.; Müller, T.; Tyuterev, V. G. *J. Phys. Chem. A* **2010**, *114*, 9927−9935.

(91) Lyakh, D. I.; Musiał, M.; Lotrich, V. F.; Bartlett, R. J. *Chem. Rev.* **2011**, *112*, 182−243.

(92) Szalay, P. G.; Müller, T.; Gidofalvi, G.; Lischka, H.; Shepard, R. *Chem. Rev.* **2011**, *112*, 108−181.

(93) Kollmar, C.; Neese, F. *J. Chem. Phys.* **2011**, *135*, 084102−084108.

(94) Mahapatra, U. S.; Chattopadhyay, S. *J. Chem. Phys.* **2011**, *134*, 044113−044122.

(95) Peyerimhoff, S. D.; Buenker, R. J. *J. Chem. Phys.* **1967**, *47*, 1953−1966.

(96) Wright, J. S. *Can. J. Chem.* **1973**, *51*, 139−146.

(97) Burton, P. G.; Harvey, M. D. *Nature* **1977**, *266*, 826−827.

(98) Burton, P. G. *Int. J. Quantum Chem.* **1977**, *12*, 207−213.

(99) Burton, P. G. *J. Chem. Phys.* **1979**, *71*, 961−972.

(100) Lucchese, R. R.; Schaefer, H. F., III. *J. Chem. Phys.* **1977**, *67*, 848−849.

(101) Timothy, J, L. *Chem. Phys. Lett.* **1990**, *169*, 529−533.

(102) Xantheas, S.; Elbert, S. T.; Ruedenberg, K. *J. Chem. Phys.* **1990**, *93*, 7519−7521.

(103) Babikov, D.; Kendrick, B. K.; Walker, R. B.; Pack, R. T.; Fleurat-Lesard, P.; Schinke, R. *J. Chem. Phys.* **2003**, *118*, 6298−6308.

(104) Kalemos, A.; Mavridis, A. *J. Chem. Phys.* **2008**, *129*, 054312−054318.

(105) De Vico, L.; Pegado, L.; Heimdal, J.; Söderhjelm, P.; Roos, B. O. *Chem. Phys. Lett.* **2008**, *461*, 136−141.

(106) Chen, J.-L.; Hu, W.-P. *J. Am. Chem. Soc.* **2011**, *133*, 16045−16053.

(107) Qu, Z. W.; Zhu, H.; Schinke, R. *J. Chem. Phys.* **2005**, *123*, 204324−204327.

(108) Shao, J.-X.; Zhu, Z.-H.; Huang, D.-H.; Wang, J.; Cheng, X.-L.; Yang, X.-D. *Chin. Phys.* **2007**, *16*, 2650.

(109) Bomble, Y. J.; Stanton, J. F.; Kallay, M.; Gauss, J. *J. Chem. Phys.* **2005**, *123*, 054101−054108.

(110) Owens, F. J. *J. Mol. Struct.: THEOCHEM* **2001**, *546*, 261−264.

(111) Gadzhiev, O. B.; Ignatov, S. K.; Gangopadhyay, S.; Masunov, A. E.; Petrov, A. I. *J. Chem. Theory Comput.* **2011**, *7*, 2021−2024.

(112) Lee, T. J.; Taylor, P. R. *Int. J. Quantum Chem.* **1989**, *36*, 199−207.

(113) Lee, T.; Rice, J.; Scuseria, G.; Schaefer, H. F., III. *Theor. Chem. Acc.* **1989**, *75*, 81−98.

(114) Hurley, A. C. *Electron Correlation in Small Molecules*; Academic: New York, 1976.

(115) Zhao, Y.; Tishchenko, O.; Gour, J. R.; Li, W.; Lutz, J. J.; Piecuch, P.; Truhlar, D. G. *J. Phys. Chem. A* **2009**, *113*, 5786−5799.

(116) Taylor, P. R. Coupled-cluster Methods in Quantum Chenistry. In *Lecture Notes in Quantum Chemistry II, Lecture Notes in Chemistry*; Roos, B. O., Ed.; Springer-Verlag: Berlin, Germany, 1994; Vol. *64*, pp 125−202.

(117) Liakos, D. G.; Neese, F. *J. Chem. Theory Comput.* **2011**, *7*, 1511−1523.

(118) Rosmus, P.; Palmieri, P.; Schinke, R. *J. Chem. Phys.* **2002**, *117*, 4871−4877.

(119) Tashiro, M.; Schinke, R. *J. Chem. Phys.* **2003**, *119*, 10186−10193.
(120) Bennett, C. J.; Kaiser, R. I. *Astrophys. J.* **2005**, *635*, 1362−1369.
(121) Sivaraman, B.; Jamieson, C. S.; Mason, N. J.; Kaiser, R. I. *Astrophys. J.* **2007**, *669*, 1414−1421.
(122) Schinke, R.; Grebenshchikov, S. Y.; Ivanov, M. V.; Fleurat-Lessard, P. *Annu. Rev. Phys. Chem.* **2006**, *57*, 625−661.
(123) Siebert, R.; Fleurat-Lessard, P.; Schinke, R.; Bittererová, M.; Farantos, S. C. *J. Chem. Phys.* **2002**, *116*, 9749−9767.
(124) Aquilanti, V.; Ascenzi, D.; Bartolomei, M.; Cappelletti, D.; Cavalli, S.; de Castro Vítores, M.; Pirani, F. *Phys. Rev. Lett.* **1999**, *82*, 69−72.
(125) Biennier, L.; Romanini, D.; Kachanov, A.; Campargue, A.; Bussery-Honvault, B.; Bacis, R. *J. Chem. Phys.* **2000**, *112*, 6309−6321.
(126) Campos-Martínez, J.; Hernández, M. I.; Bartolomei, M.; Carmona-Novillo, E.; Hernández-Lamoneda, R.; Dayou, F. Interaction and collision dynamics in O_2+O_2. In *Frontiers in Quantum Systems in Chemistry and Physics*; Wilson, S., Grout, P. J., Maruani, J., Delgado-Barrio, G., Piecuch, P., Eds.; Springer-Verlag: Berlin, Germany, 2008; pp 387−402.
(127) Slanger, T. G.; Copeland, R. A. *Chem. Rev.* **2003**, *103*, 4731−4766.
(128) Yoshida, S.; Tokuda, T.; Shimizu, K. *Appl. Phys. Lett.* **1989**, *55*, 2707−2708.
(129) Antonov, I. O.; Azyazov, V. N.; Ufimtsev, N. I. *J. Chem. Phys.* **2003**, *119*, 10638−10646.
(130) Dayou, F.; Hernández, M. I.; Campos-Martínez, J.; Hernández, R. *J. Chem. Phys.* **2005**, *123*, 074311−074312.
(131) Bussery-Honvault, B.; Veyret, V. *J. Chem. Phys.* **1998**, *108*, 3243−3248.
(132) Bartolomei, M.; Hernandez, M. I.; Campos-Martinez, J.; Carmona-Novillo, E.; Hernandez-Lamoneda, R. *Phys. Chem. Chem. Phys.* **2008**, *10*, 5374−5380.
(133) Minaev, B. F.; Nikolaev, V. D.; Ågren, H. *Spectrosc. Lett.* **1996**, *29*, 677−695.
(134) Koshi, M.; Tsuda, S.; Shimizu, K. *Mol. Simul.* **2011**, 1−10.
(135) Bahou, M.; Schriver-Mazzuoli, L.; Schriver, A. *J. Chem. Phys.* **2001**, *114*, 4045−4052.
(136) Kulikov, M. Y.; Feigin, A. M.; Ignatov, S. K.; Sennikov, P. G.; Bluszcz, T.; Schrems, O. *Atmos. Chem. Phys.* **2011**, *11*, 1729−1734.